Antiplane magneto-electro-elastic effective properties of three-phase fiber composites

CrossMark

Y. Espinosa-Almeyda [a], R. Rodríguez-Ramos [a,*], R. Guinovart-Díaz [a], J. Bravo-Castillero [a], J.C. López-Realpozo [a], H. Camacho-Montes [b], F.J. Sabina [c], F. Lebon [d]

[a] Facultad de Matemática y Computación, Universidad de La Habana, San Lázaro y L, Vedado, La Habana CP. 10400, Cuba
[b] Instituto de Ingeniería y Tecnología, Universidad Autónoma de Ciudad Juárez, Av. Del Charro 610 Norte Cd. Juárez, Chihuahua 32310, Mexico
[c] Instituto de Investigaciones en Matemáticas Aplicadas y en Sistemas, Universidad Nacional Autónoma de México, Apartado Postal 20-726, Delegación de Álvaro Obregón, 01000 México, D.F., Mexico
[d] Laboratoire de Mécanique et d'Acoustique, Université Aix-Marseille, CNRS, Centrale Marseille, 31Chemin Joseph-Aiguier, 13402 Marseille Cedex 20, France

ARTICLE INFO

ABSTRACT

In the present work, applying the asymptotic homogenization method (AHM), the derivation of the antiplane effective properties for three-phase magneto-electro-elastic fiber unidirectional reinforced composite with parallelogram cell symmetry is reported. Closed analytical expressions for the antiplane local problems on the periodic cell and the corresponding effective coefficients are provided. Matrix and inclusions materials belong to symmetry class 6mm. Numerical results are reported and compared with the eigenfunction expansion-variational method (EEVM) and other theoretical models. Good agreements are found for these comparisons. In addition, with the herein implemented solution, it is possible to reproduce the effective properties of the reduced cases such as piezoelectric or elastic composites obtaining good agreements with previous reports.

1. Introduction

Nowadays, one of the technological challenges is to build up better devices and structures that satisfy the new useful emergent technologies for getting a higher development of the mankind. In this sense, the creation of new materials is an important purpose for researchers and scientists. In this line, composite materials can potentially contribute to the search of novel materials by direct engineering of their microstructure (Jiang et al., 2004).

Magnetoelectroelastic composites is a successful case of the man-made materials, since Van Suchtelen (1972) proposed that the combination of piezoelectric-piezomagnetic phases may exhibit a new material property -the magnetoelectric coupling effect- caused by "product properties"; that is, a polarization response to an applied magnetic field, or conversely, a magnetization response to an applied electric field, through the elastic strain, (Landau and Lifshitz, 1960) showing a full coupling among magnetic, electric and mechanical fields. Because of the finding of this coupling phenomenon in a variety of microstructures and its relation to macroscopic properties several researchers have focused their attentions on this topic (Bichurin et al., 2003a,b; Lin et al., 2005; Petrov et al., 2007a,b; Singh et al., 2008, among others). There are excellent candidates for using in memory elements and smart sensor (Feng, 2009); four-state memories, magnetic field sensors, and magnetically controlled opto-electric devices (Kuo, 2011) and so on. Motivated by the above mentioned interest, the prediction of the overall properties for 'magneto-electric-elastic' (MEE) fiber composites by different micromechanical methods have been an intensive research topic.

Appropriated description for coupled properties induced from discontinuous reinforcement is still a topic of interest that have been addressed by several authors: Bracke and Van Vliet (1981), Nan (1994), Benveniste (1995), Fuentes et al. (2006), Petrov et al. (2007a,b), Tong et al. (2008) and Dinzart and Sabar (2011). Overall magneto-electro-elastic coupling properties are highly affected by the inclusions array geometry of the cell (square, hexagonal, parallelogram and randomly cell) and the interface between the constituents. For instance, two-phase fiber-reinforced composites are affected whether the phase contact is perfect or imperfect. Wang and Pan (2007), Camacho-Montes et al. (2006, 2009), Bravo-Castillero et al. (2009) and Espinosa-Almeyda et al. (2011) show

* Corresponding author. Tel.: +52 656 6884887.
E-mail addresses: yealmeyda@matcom.uh.cu (Y. Espinosa-Almeyda), reinaldo@matcom.uh.cu (R. Rodríguez-Ramos), guino@matcom.uh.cu (R. Guinovart-Díaz), jbravo@matcom.uh.cu (J. Bravo-Castillero), jclrealpozo@matcom.uh.cu (J.C. López-Realpozo), hcamacho@uacj.mx (H. Camacho-Montes), fjs@mym.iimas.unam.mx (F.J. Sabina), lebon@lma.cnrs-mrs.fr (F. Lebon).

the strong dependence of the magneto-electric coefficients on the inclusion interactions.

Considering a third phase between the matrix and the fiber can be a good idealization of the complex phenomenon that occurs at the interface. This third phase is considered as a thin layer that describes the transition zone (interphase) between the fiber and the matrix, Wang et al. (2005), Guinovart-Díaz (2008), Yan et al. (2013), etc.

In many cases of interest, the perfect interface is not an adequate model and it is necessary to include one or more interphases separating the reinforcement inclusion phase from the host matrix phase as part of the analytical model. This interphase can represent chemical interactions between the constituents, or they can be introduced by design in order to improve the properties of the composite, Guinovart-Díaz (2008). Then, a better description for imperfect bonded composites can be achieved including one or more than one extra phase between the matrix and the fiber and this proceeding transform the two phase MEE composite in a new multiphase MEE composite.

Micromechanical models used in elastic and piezoelectric problems have been extended to predict effective properties of MEE composites: The dilute (Eshelby, 1957; Zhang and Soh, 2005), self-consistent (Budiansky, 1965; Nan, 1994; Srinivas and Li, 2005), generalized self-consistent (Tong et al., 2008), differential (Mclaughlin, 1977), Mori–Tanaka (Mori and Tanaka, 1973; Benveniste, 1987; Li and Dunn, 1998; Srinivas et al., 2006; Wang and Pan, 2007) and homogenization (Benveniste and Dvorak, 1992); methods that are so used to solve the two-phase micromechanics models.

A modified Mori–Tanaka method applied on the three-phase model instead of the Eshelby's problem was proposed by Luo and Weng (1987). Also, based on the composite cylinder model and the theory of exact connections of multi-fields, the predictions of the ME coefficient was given by Benveniste (1995). The Mori–Tanaka theorem and Nemat-Nasser and Hori's multi-inclusion model is generalized by Li (2000) to analyze the heterogeneous electro-magneto-elastic solids. In those works, they take into account an inclusion containing another inclusion, which is embedded in an infinite matrix and they developed a numerical algorithm to evaluate electro-magneto-elastic Eshelby tensors.

The homogenization micromechanical method was employed to predict the effective moduli of electro-magneto-thermo-elastic multi-phase composites (Aboudi, 2001). In this method, he assumed that fields vary on multiple spatial scales due to the existence of a microstructure and the fact that the microstructure is spatially periodic.

By the finite element method (FEM), Lee et al. (2005) has investigated the effective properties of a three-phase electro-magneto-elastic composite that is composed by an elastic matrix reinforced with piezoelectric and piezomagnetic fibers. A non-zero magneto-electro-elastic coefficient is reported. Dinzart and Sabar (2011), applying the Mori–Tanaka's model obtained the effective magneto-electro-elastic properties of the composite containing thin coated inclusions. Guinovart-Díaz et al. (2013) deduced the in-plane effective properties for magneto-electro-elastic fiber unidirectional reinforced three-phase composite with square and hexagonal arrangement of cells by asymptotic homogenization method. As a generalization of the classic Rayleigh's work in 1892, Kuo (2011) developed the magnetoelectroelastic potential in multicoated elliptic fibrous composites of piezoelectric and piezomagnetic phases and performed a numerical computation for two- and three-phase transversely isotropic composites: $BaTiO_3/CoFe_2O_4$ (fibers/matrix) and $BaTiO_3$/Terfenol-D/$CoFe_2O_4$ (fiber/coated/matrix). They also reported that their results can be beneficial as design tools for functionally graded tunable composites.

Yan et al. (2013), extend the eigenfunction expansion-variational method (EEVM) reported by Yan et al. (2011) to solve the antiplane magnetoelectroelastic coupling problem for composites with a generally doubly periodic fibers array. In his work, he showed the influences of the volume fraction, permutation and the choice of the constituent phases, as well as the fiber distribution on the effective magnetoelectroelastic moduli. Besides, it is shown that the periodic array of fibers is expected to exhibit special magnetoelectric effect due to the overall anisotropy induced by general fiber arrays.

The main aim of this paper is the determination of the antiplane effective properties for three-phase magneto-electro-elastic fiber unidirectional reinforced composite with parallelogram cell symmetry using the asymptotic homogenization method (AHM), as an extension of works reported by Espinosa-Almeyda et al. (2011) and Guinovart-Díaz et al. (2013) considering perfect or imperfect conditions at the interfaces for a two-phase composite. The effect of the interphase on effective properties is receiving considerable attention in the literature and it is the motivation for this work. In general, the application of this method to a periodic medium leads necessarily to the solution of several so-called local (or canonical) problems which take place on a periodic unit cell. The present solution is mainly focused on the estimation of analytical expressions for the effective coefficients taking into account the influences of the volume fraction, permutation and the choice of the constituent phases, as well as, the fiber distribution on the effective magnetoelectroelastic moduli. In addition, the anisotropy of the composites induced by the distribution of the fibers arrays in the matrix is discussed. Numerical calculations are carried out and some comparisons with the eigenfunction expansion-variational method (EEVM) and others theoretical models are presented and good agreements are obtained.

2. Governing equations and basic formulation

A three-phase periodic composite (fiber/interphase/matrix) is considered here which consists of a parallelogram array of two circular and concentric fibers of different materials embedded in a homogeneous medium. The Cartesian coordinates system $\{O; x_1, x_2, x_3\}$ is employed for geometrical description of the composites defined in $\Omega \subset \mathbb{R}^3$. The fibers are infinitely long in the direction Ox_3 and periodically distributed. Fig. 1(a) shows the representative volume element in the plane normal $Ox_1 x_2$ to cylindrical axis. The magnetoelectroelastic material properties of each phase belong to the crystal symmetry class 6mm, where the axes of material and geometric symmetry are parallel.

The transversal sections of the periodic cell are parallelograms with two concentric circles of radius R_1 and R_2 $(R_2 < R_1)$, the phase contacts between the matrix/interphase and the interphase/fiber are considered as $\Gamma_s = \{z : z = R_s e^{i\theta}, \ 0 \leqslant \theta \leqslant 2\pi\}, (s = 1, 2)$ respectively. It is also considered the cell with periodicity property on the complex plane $z = \xi_1 + i\, \xi_2$ where ω_1 and ω_2 denote the principals periods. The region occupied for the matrix (S_1), interphase (S_2) and fiber (S_3) are respectively denoted by S_γ $(\gamma = 1, 2, 3)$ respectively, with $Y = \cup_\gamma S_\gamma$ and $\cap_\gamma S_\gamma = \varnothing$, in such way $\mathbf{x} = (x_1, x_2, x_3)$ is the global variable and $\boldsymbol{\xi} = \mathbf{x}/\varepsilon$, $\boldsymbol{\xi} = (\xi_1, \xi_2, \xi_3)$ is the quick variable, on the periodic cell Y that it is defined for a regular parallelogram in the plane $\xi_1 \xi_2$, where $\varepsilon = l/L$ is a dimensionless parameter and $L(I)$ is a linear dimension of the body (inclusion). The angle of inclination of the cell will be denoted by θ, see Fig. 1(b).

We consider magneto-electro-elastic media that exhibit linear coupling among the magnetic, electric, and elastic fields. In this case, the constitutive equations can be written in the forms, see Nan (1994):
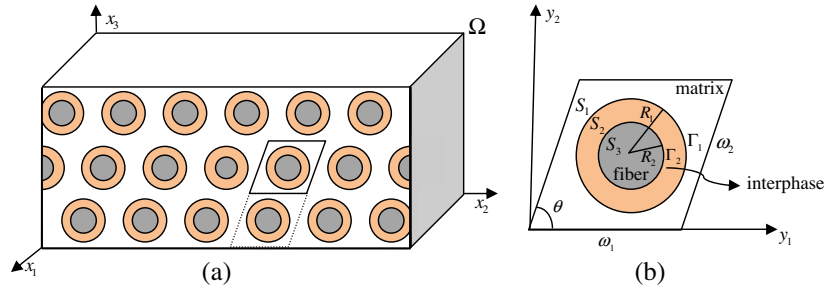
Fig. 1. (a) Cross section of a three-phase magnetoelectroelastic fiber composite with a doubly periodic microstructure and (b) extracted parallelogram periodic.

$$\sigma_{ij} = C_{ijkl}\varepsilon_{kl} - e_{kij}E_k - q_{kij}H_k, \quad D_i = e_{ikl}\varepsilon_{kl} + \kappa_{ik}E_k + \alpha_{ik}H_k,$$
$$B_i = q_{ikl}\varepsilon_{kl} + \alpha_{ik}E_k + \mu_{ik}H_k. \tag{1}$$

Also, as we are considering the static case, the Cauchy's relations as well as the relationship between the electric and magnetic fields with their respective potentials takes the following form:

$$\varepsilon_{ij} = (\partial u_i/\partial x_j + \partial u_j/\partial x_i)/2, \tag{2}$$

$$E_i = -\partial\phi/\partial x_i = -\phi_{,i} \quad H_i = -\partial\psi/\partial x_i = -\psi_{,i}. \tag{3}$$

The equilibrium and Maxwell's equations of the composites are expressed by the mechanical displacement **u** and Maxwell's quasi-static equations for electric field **E** and magnetic field **H**. They become coupled equations for **u**, **E** and **H** starting from the equations:

$$\sigma_{ij,j} = 0, \quad B_{i,i} = 0, \quad D_{i,i} = 0. \tag{4}$$

In Eqs. (1)–(4), C_{ijkl}, e_{ijk}, q_{ijk}, α_{ij}, κ_{ij} and μ_{ij} are the material properties, that denote the elastic stiffness tensor, piezoelectric, piezomagnetic and magneto-electric coupling tensors, the dielectric permittivities and the magnetic permeabilities, respectively. σ_{ij}, D_i, B_i, ε_{kl}, E_k and H_k denote the components of the stress, electric displacement, magnetic induction, strain, electric and magnetic fields respectively, and we use u_k, ϕ and ψ to represent the displacement component, the electric and the magnetic potentials. The summation convention over repeated Latin indices is understood and i, j, k and l run from 1 to 3 and the comma represents the partial derivative respect to the correspondent variable. Also, the material properties satisfy the following symmetries: $C_{ijkl} = C_{jikl} = C_{ijlk} = C_{klij}$, $e_{kij} = e_{kji}$, $q_{kij} = q_{kji}$, $\kappa_{ik} = \kappa_{ki}$, $\alpha_{ik} = \alpha_{ki}$, $\mu_{ik} = \mu_{ki}$ and the positivity conditions

$$\exists \eta_1 > 0, \quad \forall \mathcal{X} \in \mathbb{E}_s^3, \quad C_{ijkl}(\mathbf{x}/\varepsilon)\mathcal{X}_{ij}\mathcal{X}_{kl} \geqslant \eta_1 \mathcal{X}_{ij}\mathcal{X}_{kl},$$
$$\exists \eta_2 > 0, \quad \forall \mathbf{a} \in \mathbb{R}^3, \quad \kappa_{ik}(\mathbf{x}/\varepsilon)a_i a_k \geqslant \eta_2 a_i a_k,$$
$$\exists \eta_3 > 0, \quad \forall \mathbf{b} \in \mathbb{R}^3, \quad \mu_{ik}(\mathbf{x}/\varepsilon)b_i b_k \geqslant \eta_3 b_i b_k,$$

where η_1, η_2, η_3 are positive constants and $\mathbb{E}_s^3$ is the space of symmetric 3×3 matrices.

Substituting (1)–(3) into (4) we obtain a system of partial differential equations with rapidly oscillating coefficients on the region Ω,

$$(C_{ijlk}(y)u_{l,k} + e_{kij}(y)\phi_{,k} + q_{kij}(y)\psi_{,k})_j = 0,$$
$$(e_{kij}(y)u_{i,k} - \kappa_{jk}(y)\phi_{,k} - \alpha_{jk}(y)\psi_{,k})_j = 0, \tag{5}$$
$$(q_{kij}(y)u_{i,k} - \alpha_{jk}(y)\phi_{,k} - \mu_{jk}(y)\psi_{,k})_j = 0,$$

which constitute the system of fundamental equations of the theory of the linear magneto-electro-elasticity for a heterogeneous structure Ω. The problem is to solve (5) subject to the boundary conditions:

$$u|_{\partial\Omega} = g_1(x), \quad \phi|_{\partial\Omega} = g_2(x), \quad \psi|_{\partial\Omega} = g_3(x), \tag{6}$$

where $g_1(x)$, $g_2(x)$ and $g_3(x)$ are infinity differentiable functions on Ω.

In a two-dimensional situation, like the herein considered geometry, it turns out that the above equations uncouple into two independent systems under suitable boundary conditions. Just like, the familiar plane- and anti-plane-strain deformation states in linear elasticity, see Camacho-Montes et al. (2006, 2009) and López-López et al. (2005). In the state of in-plane mechanical deformation and out-of-plane electric and magnetic fields, the mechanical displacements u_1, u_2 and the fields E_3, B_3 are involved. The other state, which is of particular interest in this work, it is the anti-plane mechanical deformation and in-plane electric and magnetic fields. Here, the mechanical displacement u_3 and the electric and magnetic fields E_1, E_2, H_1 and H_2 are the involved variables, see Chen (1993), Benveniste (1995) and Kuo (2011) by:

$$u_1 = u_2 = 0, \quad u_3 = u_3(x,y), \quad \phi = \phi(x,y), \quad \psi = \psi(x,y), \tag{7}$$

where u_1, u_2, u_3 are the mechanical displacements along the O_x, O_y and O_z axes, ϕ and ψ are the electric and magnetic potentials, respectively.

In addition to Eqs. (1)–(6), we have to use interface conditions between the two contiguous phases, occupied by S_γ, these interface conditions are assumed to be in perfect contact along the interfaces Γ_s of each cylinder. The displacement, quasi-static electric and magnetic potentials, traction, normal electric displacement and normal magnetic induction are continuous across the interfaces Γ_s, between the phases. Therefore the perfect contact condition can be written as:

$$\|u_i\|_s = 0, \quad \|\phi\|_s = 0, \quad \|\psi\|_s = 0, \tag{8}$$

$$\|\sigma_{ij}n_j\|_s = 0, \quad \|D_i n_i\|_s = 0, \quad \|B_i n_i\|_s = 0, \tag{9}$$

the double bar notation $\|f\|_s$ is used to denote the jump of the relevant function f across the interphase Γ_s, i.e. $\|f\|_1 = f^{(1)} - f^{(2)}$ and $\|f\|_2 = f^{(2)} - f^{(3)}$, whereas the indices (1)–(3) denotes the matrix, the interphase and the fiber properties respectively. n_i is the component of the outward unit normal vector **n** to the interface Γ_s.

3. Method of solution

By means of the well-known asymptotic homogenization method reported by Rodríguez-Ramos et al. (2001) and Pobedrya (1984), it is possible to obtain from (1)–(6) an asymptotic solution of the above statement of the problem, the local problems on the periodic cell and the effective coefficients analogous to those reported in Espinosa-Almeyda et al. (2011), being this, the main aim of this work. The solutions can be solved asymptotically posing the ansatz:

$$u_3(x) = w_0(x,y) + \varepsilon w_1(x,y) + O(\varepsilon^2), \tag{10}$$

$$\phi(x) = \phi_0(x,y) + \varepsilon\phi_1(x,y) + O(\varepsilon^2), \tag{11}$$

$$\psi(x) = \psi_0(x, y) + \varepsilon\psi_1(x, y) + O(\varepsilon^2) \tag{12}$$

and stating the two scales. The functions w_0, w_1, ϕ_0, ϕ_1, ψ_0 and ψ_1 are found to satisfy certain differential equations related to the original system in a unit cell (see Fig. 1) with periodic conditions, also they are infinitely differentiable and Y-periodic with respect to the fast variable ξ. It is a well-known derivation whose details can be found elsewhere (e.g., Parton and Kudryavtsev, 1993) and here is omitted.

Of a greater interest are the so-called local (or canonical) problems associated here with the correction terms w_1, ϕ_1 and ψ_1 to the mean variations w_0, ϕ_0 and ψ_0 respectively, since they appear in the formulae of the effective properties. Due to the linearity of the main equations on the antiplane case, the corrections terms w_1, ϕ_1 and ψ_1 can be obtained as a linear combination of some of such displacements and potentials. This, however, will not be done here, since the main objective of this paper is the characterization of the effective properties.

Twelve local problems arise $_{\alpha q}\mathcal{L}$, $_\alpha\mathcal{I}$ and $_q\mathcal{P}$ ($\alpha = 1, 2$; $q = 1, 2, 3$) over the periodic unit cell Y, defined bellow (see for instance Parton and Kudryavtsev, 1993). Only six local problems out of these twelve are defined as antiplane problem, see Camacho-Montes et al. (2009) and Espinosa-Almeyda et al. (2011), which are referred as $_{13}\mathcal{L}$, $_{23}\mathcal{L}$, $_1\mathcal{I}$, $_2\mathcal{I}$, $_1\mathcal{P}$ and $_2\mathcal{P}$. A pre-index is used to distinguish similar constants and functions such as displacements and potentials, which appear below. Considering also, that each homogeneous phase is a material with 6mm symmetry, in connection with the antiplane local problems previously reported the corresponding effective coefficients are: C^*_{1313}, C^*_{3213}, e^*_{113}, e^*_{213}, q^*_{113}, q^*_{213}, κ^*_{11}, κ^*_{21}, α^*_{11}, α^*_{21}, μ^*_{12} and μ^*_{22}.

4. Antiplane local problems $_{\alpha3}L$, ($\alpha = 1, 2$)

For simplicity, only the main results of the local problem $_{\alpha3}\mathcal{L}$, are shown. The mathematical statement of local problems $_{\alpha3}\mathcal{L}$ is now formulated and the fundamental problem consists in finding the corresponding functions $_{\alpha3}\mathcal{L}_3^{(\gamma)}$, $_{\alpha3}\mathcal{M}^{(\gamma)}$ and $_{\alpha3}\mathcal{N}^{(\gamma)}$ that satisfies the Laplace equations, the perfect conditions at the interfaces Γ_s and the null average over the periodic cell, takes the following form:

$$\left(C^{(\gamma)}_{ij3l}{}_{\alpha3}\mathcal{L}^{(\gamma)}_{3,l} + e^{(\gamma)}_{lij}{}_{\alpha3}\mathcal{M}^{(\gamma)}_{,l} + q^{(\gamma)}_{lij}{}_{\alpha3}\mathcal{N}^{(\gamma)}_{,l}\right)_j = -\left(C^{(\gamma)}_{ij\alpha3}\right)_j,$$

$$\left(e^{(\gamma)}_{i3l}{}_{\alpha3}\mathcal{L}^{(\gamma)}_{3,l} - \kappa^{(\gamma)}_{il}{}_{\alpha3}\mathcal{M}^{(\gamma)}_{,l} - \alpha^{(\gamma)}_{il}{}_{\alpha3}\mathcal{N}^{(\gamma)}_{,l}\right)_j = -\left(e^{(\gamma)}_{i\alpha3}\right)_j, \tag{13}$$

$$\left(q^{(\gamma)}_{i3l}{}_{\alpha3}\mathcal{L}^{(\gamma)}_{3,l} - \alpha^{(\gamma)}_{il}{}_{\alpha3}\mathcal{M}^{(\gamma)}_{,l} - \mu^{(\gamma)}_{il}{}_{\alpha3}\mathcal{N}^{(\gamma)}_{,l}\right)_j = -\left(q^{(\gamma)}_{i\alpha3}\right)_j, \quad \text{in} \quad Y,$$

$$\|_{\alpha3}\mathcal{L}_3\|_s = 0, \quad \|_{\alpha3}\mathcal{M}\|_s = 0, \quad \|_{\alpha3}\mathcal{N}\|_s = 0, \quad \text{on} \quad \Gamma_s, \tag{14}$$

$$\|_{\alpha3}\sigma_{ij}n_j\|_s = -\|C_{ij\alpha3}\|n_j,$$

$$\|_{\alpha3}D_jn_j\|_s = -\|e_{j\alpha3}\|n_j, \tag{15}$$

$$\|_{\alpha3}B_jn_j\|_s = -\|q_{j\alpha3}\|n_j, \quad \text{on} \quad \Gamma_s,$$

$$\langle_{\alpha3}\mathcal{L}_3\rangle = \langle_{\alpha3}\mathcal{M}\rangle = \langle_{\alpha3}\mathcal{N}\rangle = 0, \tag{16}$$

where $_{\alpha3}\sigma^{(s)}_{ij} = C^{(s)}_{ij3l}{}_{\alpha3}\mathcal{L}^{(s)}_{3,l} + e^{(s)}_{lij}{}_{\alpha3}\mathcal{M}^{(s)}_{,l} + q^{(s)}_{lij}{}_{\alpha3}\mathcal{N}^{(s)}_{,l}$, $_{\alpha3}D^{(s)}_j = e^{(s)}_{j3l}{}_{\alpha3}\mathcal{L}^{(s)}_{3,l} - \kappa^{(s)}_{lj}{}_{\alpha3}\mathcal{M}^{(s)}_{,l} - \alpha^{(s)}_{lj}{}_{\alpha3}\mathcal{N}^{(s)}_{,l}$, $_{\alpha3}B^{(s)}_j = q^{(s)}_{j3l}{}_{\alpha3}\mathcal{L}^{(s)}_{3,l} - \alpha^{(s)}_{lj}{}_{\alpha3}\mathcal{M}^{(s)}_{,l} - \mu^{(s)}_{lj}{}_{\alpha3}\mathcal{N}^{(s)}_{,l}$ and the angular bracket define the volume average per unit length over the area V of the cell, that is,

$$\langle F\rangle = \frac{1}{V}\int_V F(\xi)d\xi \tag{17}$$

being $_{\alpha3}\mathcal{L}_3$, $_{\alpha3}\mathcal{M}$ and $_{\alpha3}\mathcal{N}$ the local functions corresponding to the mechanical displacements, the electric potentials and the magnetic potentials associated to the present local problems with $\alpha = 1, 2$. The subscripts before the local functions will be omitted for simplicity of the expressions.

Thus, the functions $\mathcal{L}_3$, $\mathcal{M}$ and $\mathcal{N}$ are sought in such a way that they also are doubly periodic harmonic functions of the complex variable $z = y_1 + iy_2$ in the periodic cell Y, with the periods $\omega_1 = 1$ and $\omega_2 = e^{i\theta}$ where $\theta = \pi/2$ for square symmetry and $\theta = \pi/3$ for hexagonal symmetry and another case for parallelogram symmetry (see Fig. 1(b)). Now, the comma notation represents the partial derivate relative the local variable ξ_l.

5. Solution of the local problems $_{\alpha3}\mathcal{L}$, ($\alpha = 1, 2$)

Considering the mathematical statement of the present problems, doubly periodic harmonic functions $\mathcal{L}_3$, $\mathcal{M}$ and $\mathcal{N}$ are to be found in terms of the following Laurent expansions of harmonic functions over the region S_1,

$$\mathcal{L}_3^{(1)}(z) = \text{Re}\left\{\frac{a_0z}{R_1} + \sum_{p=1}^{\infty}{}^o a_p\frac{R_1^p}{z^p} + \sum_{p=1}^{\infty}{}^o\sum_{k=1}^{\infty}{}^o a_k\sqrt{\frac{k}{p}}w_{kp}\frac{z^p}{R_1^p}\right\}$$
$$= \text{Re}\left\{\frac{a_0z}{R_1} + \sum_{k=1}^{\infty}{}^o a_kR_1^k\frac{\zeta^{(k-1)}(z)}{(k-1)!}\right\},$$

$$\mathcal{M}^{(1)}(z) = \text{Re}\left\{\frac{b_0z}{R_1} + \sum_{p=1}^{\infty}{}^o b_p\frac{R_1^p}{z^p} + \sum_{p=1}^{\infty}{}^o\sum_{k=1}^{\infty}{}^o b_k\sqrt{\frac{k}{p}}w_{kp}\frac{z^p}{R_1^p}\right\}$$
$$= \text{Re}\left\{\frac{b_0z}{R_1} + \sum_{k=1}^{\infty}{}^o b_kR_1^k\frac{\zeta^{(k-1)}(z)}{(k-1)!}\right\}, \tag{18}$$

$$\mathcal{N}^{(1)}(z) = \text{Re}\left\{\frac{e_0z}{R_1} + \sum_{p=1}^{\infty}{}^o e_p\frac{R_1^p}{z^p} + \sum_{p=1}^{\infty}{}^o\sum_{k=1}^{\infty}{}^o e_k\sqrt{\frac{k}{p}}w_{kp}\frac{z^p}{R_1^p}\right\}$$
$$= \text{Re}\left\{\frac{e_0z}{R_1} + \sum_{k=1}^{\infty}{}^o e_kR_1^k\frac{\zeta^{(k-1)}(z)}{(k-1)!}\right\},$$

where $w_{kp} = \frac{(k+p-1)!}{(k-1)!(p-1)!}\frac{R_1^{k+p}}{\sqrt{kp}}S_{k+p}$, $S_{k+p} = \sum_{m,n}(m\omega_1 + n\omega_2)^{-(k+p)}$, $m^2 + n^2 \neq 0$, $k + l > 2$ and $S_2 = 0$.

By the sum of the power expansions over the region S_2

$$\mathcal{L}_3^{(2)}(z) = \text{Re}\left\{\sum_{p=1}^{\infty}{}^o a^{(2)}_{-p}\frac{R_1^p}{z^p} + \sum_{p=1}^{\infty}{}^o a^{(2)}_p\frac{z^p}{R_2^p}\right\},$$

$$\mathcal{M}^{(2)}(z) = \text{Re}\left\{\sum_{p=1}^{\infty}{}^o b^{(2)}_{-p}\frac{R_1^p}{z^p} + \sum_{p=1}^{\infty}{}^o b^{(2)}_p\frac{z^p}{R_2^p}\right\},$$

$$\mathcal{N}^{(2)}(z) = \text{Re}\left\{\sum_{p=1}^{\infty}{}^o e^{(2)}_{-p}\frac{R_1^p}{z^p} + \sum_{p=1}^{\infty}{}^o e^{(2)}_p\frac{z^p}{R_2^p}\right\} \tag{19}$$

and power expansions over the region S_3,

$$\mathcal{L}_3^{(3)}(z) = \text{Re}\left\{\sum_{k=1}^{\infty}{}^o c_k\frac{z^k}{R_2^k}\right\}, \quad \mathcal{M}^{(3)}(z) = \text{Re}\left\{\sum_{k=1}^{\infty}{}^o d_k\frac{z^k}{R_2^k}\right\},$$

$$\mathcal{N}^{(3)}(z) = \text{Re}\left\{\sum_{k=1}^{\infty}{}^o f_k\frac{z^k}{R_2^k}\right\}, \tag{20}$$

where the symbols Re or Im are the real or imaginary part of the complex number, respectively, R_1 and R_2 ($R_2 < R_1$) are the radiuses of the fibers in the composites. a_0, a_k, $a^{(2)}_p$, $a^{(2)}_{-p}$, b_0, b_k, $b^{(2)}_p$, $b^{(2)}_{-p}$, e_0, e_k, $e^{(2)}_p$, $e^{(2)}_{-p}$, c_k, d_k, f_k are complex undetermined coefficients which depend on the local problems $_{\alpha3}\mathcal{L}$ to be solved and the superscript "o" next to the summation symbol means that "k" runs only over odd integers. ζ is the Zeta quasi periodic Weierstrass function defined as $\zeta(z) = \frac{1}{z} + \sum'_{m,n}\{\frac{1}{z-\beta_{mn}} + \frac{1}{\beta_{mn}} + \frac{z}{\beta_{mn}^2}\}$ that satisfied the quasi periodic conditions $\delta_\gamma = \zeta(z + \omega_\gamma) - \zeta(z)$, being $\beta_{mn} = m\omega_1 + n\omega_2$, with ω_1 and ω_2 the principal periods and for $m, n \in \mathbb{Z}$ the prime over the summation symbol means that the pair $(m, n) = (0, 0)$ is excluded.

Substituting the previous expansion (18)–(20) into the contact conditions at the interface (Eq. (15)), after some algebraic manipulations, we obtain an infinite systems that are transformed into dimensionless equations to facilitate solution by means of the following relations defined in Appendix A, see Wang and Ding (2006):

$$
\begin{pmatrix} \mathcal{A}_{1p} & \mathcal{B}_{1p} & \mathcal{C}_{1p} \\ \mathcal{A}_{3p} & \mathcal{B}_{3p} & \mathcal{C}_{3p} \\ \mathcal{A}_{5p} & \mathcal{B}_{5p} & \mathcal{C}_{5p} \end{pmatrix} \begin{pmatrix} \bar{a}_p \\ \bar{b}_p \\ \bar{e}_p \end{pmatrix} + \begin{pmatrix} \mathcal{A}_{2p} & \mathcal{B}_{2p} & \mathcal{C}_{2p} \\ \mathcal{A}_{4p} & \mathcal{B}_{4p} & \mathcal{C}_{4p} \\ \mathcal{A}_{6p} & \mathcal{B}_{6p} & \mathcal{C}_{6p} \end{pmatrix} \begin{pmatrix} E_p(a) \\ E_p(b) \\ E_p(e) \end{pmatrix}
$$
$$
= \begin{pmatrix} \mathcal{T}_{1p} \\ \mathcal{T}_{2p} \\ \mathcal{T}_{3p} \end{pmatrix} \delta_{1p}[\delta_{\alpha 1} - i\delta_{\alpha 2}], \tag{21}
$$

where the following notation is introduced $E_p(\bullet) = (\bullet)_0 \delta_{1p} - \sum_{k=1}^{\infty} {}^o(\bullet)_k \sqrt{kp^{-1}} w_{kp}$, $(\bullet) = (a, b, e)$ and the complex unknown constants a_p, b_p and e_p, and their conjugate denoted by the over bar are the solutions of the corresponding local problems $_{\alpha 3}\mathcal{L}$. Here, the sum by the repeated indices k and p are applied, with $k, p = 1, 3, 5, \ldots$, δ_{1p} is the Kronecker's delta and the constants $\mathcal{A}_{ip}$, $\mathcal{B}_{ip}$, $\mathcal{C}_{ip}$, $\mathcal{T}_{1p}$, $\mathcal{T}_{2p}$ and $\mathcal{T}_{3p}$ are defined in Appendix B. The solutions of the system of each local problem depend on the material constants, geometry of the fibers and the different fields related to the problem.

From the condition of double periodicity of the functions $\mathcal{L}_3$, $\mathcal{M}$ and $\mathcal{N}$ the following relations we can concluded: $a_0 = -R_1^2 \tilde{H}_2 a_1 - R_1^2 \tilde{H}_1 \bar{a}_1$, $b_0 = -R_1^2 \tilde{H}_2 b_1 - R_1^2 \tilde{H}_1 \bar{b}_1$, $e_0 = -R_1^2 \tilde{H}_2 e_1 - R_1^2 \tilde{H}_1 \bar{e}_1$, where $\tilde{H}_1 = (\bar{\delta}_1 \bar{\omega}_2 - \bar{\delta}_2 \bar{\omega}_1)/(\omega_1 \bar{\omega}_2 - \omega_2 \bar{\omega}_1)$ and $\tilde{H}_2 = (\delta_1 \bar{\omega}_2 - \delta_2 \bar{\omega}_1)/(\omega_1 \bar{\omega}_2 - \omega_2 \bar{\omega}_1)$.

Also, analogous to Guinovart-Díaz et al. (2011), introducing in Eq. (21) the following set of variables is defined: $a_k = (x_k + iy_k)/\sqrt{k}$, $b_k = (z_k + it_k)/\sqrt{k}$, $e_k = (l_k + im_k)/\sqrt{k}$, $w_{kp} = w_{1kp} + iw_{2kp}$, $\tilde{H}_\alpha = h_{1\alpha} + ih_{2\alpha}$, being x_k, y_k, z_k, t_k, l_k, m_k, w_{1kp}, w_{2kp}, $h_{1\alpha}$ and $h_{2\alpha}$ real numbers, that represent the real or imaginary part of the previously complex numbers and $i = \sqrt{-1}$. After some algebraic manipulations, the solution of above equation system (21) can be rewritten in the following matrix form:

$$
X = \left[\left(\tilde{E}_1 + R_1^2 J \right) - N_1 (\tilde{E} + W)^{-1} N_2 \right]^{-1} B, \tag{22}
$$

where $\tilde{E}_1$, J are square matrices of order 6, $\tilde{E}$ and W are the order $6N$ formed by six order blocks $\tilde{E}_p$ and W_{kp} respectively, defined in Appendix C, here k and p are odd numbers. The matrix $N_1 = W_{k1}$, $N_2 = W_{1p}$ are the order $6 \times 6N$ and $6N \times 6$ respectively. $N \in \mathbb{N}$ is the truncate order of the system (21). Also, $X^T = (x_1, y_1, z_1, t_1, l_1, m_1, \ldots, x_k, y_k, z_k, t_k, l_k, m_k, \ldots)$ is the transpose of vector X and $B^T = (\mathcal{T}_{11}\delta_{\alpha 1}, \mathcal{T}_{11}\delta_{\alpha 2}, \mathcal{T}_{21}\delta_{\alpha 1}, \mathcal{T}_{21}\delta_{\alpha 2}, \mathcal{T}_{31}\delta_{\alpha 1}, \mathcal{T}_{31}\delta_{\alpha 2}, 0, 0, 0, 0, 0, 0, \ldots)$ is the transpose of vector B, both infinite vectors.

From Eq. (22), a very important first approximation is obtained if we consider $x_k = y_k = z_k = t_k = l_k = m_k = 0$ for $k \geq 3$, in this case the unknowns with subscript $p = k = 1$ remain no null. This approximation is equivalent to truncate the equation system (21) to an appropriate order N, which denotes the number of equations considered in the solution of the infinite algebraic system of equation, particularly to $N = 1$ (short formulae). It is solved and its solution is:

$$
X_1 = \left[\left(\tilde{E}_1 + R_1^2 J \right) - N_1 (\tilde{E}_p + W)^{-1} N_2 \right]^{-1} B_1, \tag{23}
$$

where $X_1^T = (x_1 \quad y_1 \quad z_1 \quad t_1 \quad l_1 \quad m_1)$ and $B_1^T = (\mathcal{T}_{11}\delta_{\alpha 1} \quad \mathcal{T}_{11}\delta_{\alpha 2} \quad \mathcal{T}_{21}\delta_{\alpha 1} \quad \mathcal{T}_{21}\delta_{\alpha 2} \quad \mathcal{T}_{31}\delta_{\alpha 1} \quad \mathcal{T}_{31}\delta_{\alpha 2})$.

In general, using the solution of the equation system (23), we can obtained the constant $a_1 = x_1 + iy_1$, $b_1 = z_1 + it_1$ and $e_1 = l_1 + im_1$, that are essential for the effective coefficients

associate with these local problems $_{\alpha 3}\mathcal{L}$. The same method used for solving the local problem $_{\alpha 3}\mathcal{L}$ ($\alpha = 1, 2$) may be developed to solve the other antiplane shear local problems $_1\mathcal{I}$, $_2\mathcal{I}$, $_1\mathcal{P}$ and $_2\mathcal{P}$. These problems are very similar to $_{\alpha 3}\mathcal{L}$.

6. Effective coefficients

The main objective of this work is the characterization of the effective properties for three-phase magneto-electro-elastic fiber unidirectional reinforced composite with parallelogram cell. Then, the corresponding effective coefficients related to the local problems $_{\alpha 3}\mathcal{L}$ are shown.

Effective coefficients associate with the local problem $_{13}\mathcal{L}$

$$
C_{1313}^* = \langle C_{1313} \rangle + \langle C_{1331} \mathscr{L}_{3,1} \rangle + \langle e_{113} \mathscr{M}_{,1} \rangle + \langle q_{113} \mathscr{N}_{,1} \rangle,
$$
$$
C_{2313}^* = \langle C_{2332} \mathscr{L}_{3,2} \rangle + \langle e_{223} \mathscr{M}_{,2} \rangle + \langle q_{223} \mathscr{N}_{,2} \rangle,
$$

$$
e_{113}^* = \langle e_{113} \rangle + \langle e_{131} \mathscr{L}_{3,1} \rangle - \langle \kappa_{11} \mathscr{M}_{,1} \rangle - \langle \alpha_{11} \mathscr{N}_{,1} \rangle,
$$
$$
e_{213}^* = \langle e_{113} \mathscr{L}_{3,2} \rangle - \langle \kappa_{11} \mathscr{M}_{,2} \rangle - \langle \alpha_{11} \mathscr{N}_{,2} \rangle, \tag{24}
$$

$$
q_{113}^* = \langle q_{113} \rangle + \langle q_{131} \mathscr{L}_{3,1} \rangle - \langle \alpha_{11} \mathscr{M}_{,1} \rangle - \langle \mu_{11} \mathscr{N}_{,1} \rangle,
$$
$$
q_{213}^* = \langle q_{113} \mathscr{L}_{3,2} \rangle - \langle \alpha_{11} \mathscr{M}_{,2} \rangle - \langle \mu_{11} \mathscr{N}_{,2} \rangle.
$$

Effective coefficients associate with the local problem $_{23}\mathcal{L}$

$$
C_{1323}^* = \langle C_{1331} \mathscr{L}_{3,1} \rangle + \langle e_{113} \mathscr{M}_{,1} \rangle + \langle q_{113} \mathscr{N}_{,1} \rangle,
$$
$$
C_{2323}^* = \langle C_{1313} \rangle + \langle C_{1313} \mathscr{L}_{3,2} \rangle + \langle e_{113} \mathscr{M}_{,2} \rangle + \langle q_{113} \mathscr{N}_{,2} \rangle,
$$

$$
e_{123}^* = \langle e_{131} \mathscr{L}_{3,1} \rangle - \langle \kappa_{11} \mathscr{M}_{,1} \rangle - \langle \alpha_{11} \mathscr{N}_{,1} \rangle,
$$
$$
e_{223}^* = \langle e_{223} \rangle + \langle e_{113} \mathscr{L}_{3,2} \rangle - \langle \kappa_{11} \mathscr{M}_{,2} \rangle - \langle \alpha_{11} \mathscr{N}_{,2} \rangle, \tag{25}
$$

$$
q_{123}^* = \langle q_{131} \mathscr{L}_{3,1} \rangle - \langle \alpha_{11} \mathscr{M}_{,1} \rangle - \langle \mu_{11} \mathscr{N}_{,1} \rangle,
$$
$$
q_{223}^* = \langle q_{113} \rangle + \langle q_{113} \mathscr{L}_{3,2} \rangle - \langle \alpha_{11} \mathscr{M}_{,2} \rangle - \langle \mu_{11} \mathscr{N}_{,2} \rangle.
$$

The local functions $\mathscr{L}_3$, $\mathscr{M}$ and $\mathscr{N}$ are the solutions of the local problems $_{\alpha 3}\mathcal{L}$, respectively. The expressions of the effective coefficients (24) and (25) are transformed applying Green's theorem to the area integrals. Subsequently, substituting the previous expansion (18)–(20) into the lineal integrals and using the orthogonality of the system of functions $\{\cos(nx), sen(nx)\}_{n=-\infty}^{\infty}$ in $[0, 2\pi]$ and making the transformations shown in Appendix D, the analytical expressions of the dimensionless effective properties are obtained as functions of the unknown constants $\bar{a}_1$, $\bar{b}_1$ and $\bar{e}_1$, associated to each local problems $_{13}\mathcal{L}$ or $_{23}\mathcal{L}$, as follows:

$$
C_{1313}^* - iC_{2313}^* = C_{1313} + \Upsilon_1 \bar{a}_1 + \Upsilon_2 \bar{b}_1 + \Upsilon_3 \bar{e}_1 + \Delta_1,
$$
$$
e_{113}^* - ie_{213}^* = e_{113} + \Upsilon_4 \bar{a}_1 - \Upsilon_5 \bar{b}_1 - \Upsilon_6 \bar{e}_1 + \Delta_2, \quad \text{in local problem } _{13}\mathcal{L}
$$
$$
q_{113}^* - iq_{213}^* = q_{113} + \Upsilon_7 \bar{a}_1 - \Upsilon_8 \bar{b}_1 - \Upsilon_9 \bar{e}_1 + \Delta_3; , \tag{26}
$$

$$
C_{1323}^* - iC_{2323}^* = -iC_{2323} + \Upsilon_1 \bar{a}_1 + \Upsilon_2 \bar{b}_1 + \Upsilon_3 \bar{e}_1 - i\Delta_1,
$$
$$
e_{123}^* - ie_{223}^* = -ie_{223} + \Upsilon_4 \bar{a}_1 - \Upsilon_5 \bar{b}_1 - \Upsilon_6 \bar{e}_1 - i\Delta_2, \quad \text{in local problem } _{23}\mathcal{L}
$$
$$
q_{123}^* - iq_{223}^* = -iq_{223} + \Upsilon_7 \bar{a}_1 - \Upsilon_8 \bar{b}_1 - \Upsilon_9 \bar{e}_1 - i\Delta_3, \tag{27}
$$

with $C_{1313} = (C_{1313})_v/C_{1313}^{(1)}$, $e_{113} = (e_{113})_v/\sqrt{C_{1313}^{(1)}\kappa_{11}^{(1)}}$ and $q_{113} = (q_{113})_v/\sqrt{C_{1313}^{(1)}\mu_{11}^{(1)}}$. Also, $(f)_v = f^{(1)}V_1 + f^{(2)}V_2 + f^{(3)}V_3$, where V_1, V_2 and V_3 are the volume fraction per unit length occupied by the matrix, interphase and the fiber, respectively; $V_1 + V_2 + V_3 = 1$ and $V = |\omega_1||\omega_2|\sin\theta$ represent the volume of periodic cell. The coefficients Υ_m $m = \overline{1, 9}$, and Δ_i ($i = 1, 2, 3$) are defined in Appendix D.

Analogously, the remaining dimensionless effective properties from the antiplane local problems $_1\mathcal{I}$, $_2\mathcal{I}$, $_1\mathcal{P}$ and $_2\mathcal{P}$ can be calculated. They are listed as follows,

$$e^*_{113}, \ e^*_{123}, \ \kappa^*_{11}, \ \kappa^*_{21}, \ \alpha^*_{11} \quad \text{and} \quad \alpha^*_{21} \text{ associated with } _1\mathcal{I}, \tag{28}$$

$$e^*_{213}, \ e^*_{223}, \ \kappa^*_{12}, \ \kappa^*_{22}, \ \alpha^*_{12} \quad \text{and} \quad \alpha^*_{22} \text{ associated with } _2\mathcal{I}, \tag{29}$$

$$q^*_{113}, \ q^*_{123}, \ \alpha^*_{11}, \ \alpha^*_{21}, \ \mu^*_{11} \quad \text{and} \quad \mu^*_{21} \text{ associated with } _1\mathcal{P}, \tag{30}$$

$$q^*_{213}, \ q^*_{223}, \ \alpha^*_{12}, \ \alpha^*_{22}, \ \mu^*_{12} \quad \text{and} \quad \mu^*_{22} \text{ associated with } _2\mathcal{P}. \tag{31}$$

To have the remaining effective properties, it will be only necessary to solve the associated local problems $_\alpha\mathcal{I}$ and $_q\mathcal{P}$. The unknowns $\bar{a}_1$, $\bar{b}_1$ and $\bar{c}_1$ are different for each individual local problem and they are obtained from the system of equation (22) using the corresponding independent terms related to each local problems. The dimensions can be retrieved in the inverse form using the transformations of Appendix A.

7. Numerical results

In the present work, it is investigated the influences of the volume fraction, fiber distribution and phase permutation on the effective magnetoelectroelastic moduli considering the volume cell illustrated in Fig. 1. Two different cases: **a two-phase Model** (fiber/matrix = BaTiO₃/CoFe₂O₄) and a **three-phase Model** (fiber/interphase/matrix = BaTiO₃/Terfenol-D/CoFe₂O₄) are taking into consideration for numerical simulations.

The analytical expressions of the effective properties (26) and (27) are in function of the material properties, the volume fraction and the residues a_1, b_1 and e_1 of the functions (18). The system in Eq. (23) is truncated to N order and solved for a_1, b_1 and e_1. This procedure is repeated for different orders. For each N, new solutions a_1, b_1 and e_1 are obtained and compared to the ones of the preceding step. Calculation stops when the difference between these coefficients for subsequent steps reaches the desired precision. The coefficients a_1, b_1 and e_1 are substituted into (26) and (27) in order to finally obtain the overall properties. Only a few iterations are needed to achieve the convergence.

An important result is that the approach in Eq. (23) for $N = 1$ reproduces exactly the values that are determined by Mori–Tanaka

self-consistent method reported in Wang and Pan (2007), when considering a three-phase model with very thin interphase.

From the present three-phase model, it can be obtained the analytical expressions of the composite without interphase (two phase composite) reported in previously works by Camacho-Montes et al. (2009). In addition, limit cases can be verified and the analytical expressions can be reduced to those reported for transversally isotropic bi- or three-phase composites, with elastic or piezoelectric constituents and square, hexagonal, parallelogram cells, such as, Guinovart-Díaz et al. (2011, 2012), Rodríguez-Ramos et al. (2011).

The aforementioned global properties of the antiplane behavior of the two- or three-phase magneto-electro-elastic fibrous composite as function of the cell's constituents are calculated considering the constitutive properties shows in Table 1 (see Yan et al., 2013). For simplicity, the two index notation, in the expression of the effective properties, is used in tables and figures.

The numerical validity and efficient of the herein developed analytical results by means of the asymptotic homogenization method (AHM) are verified by comparing them with the other ones published by Yan et al. (2013) (EEVM, i.e., eigenfunction expansion-variational method) and by Kuo (2011), who combined the methods of complex potentials with a re-expansion formulae and the generalized Rayleigh's formulation. The parameter $\lambda = V_3$ is defined as the fiber volume fraction for a two-phase composite and $\lambda = V_2 + V_3$ is the volume fraction of the fiber and interphase together for a three-phase composite. For both cases $1 - \lambda$ is the matrix volume fraction. In this example, the concentric fibers radius relation is $R_2/R_1 = 4/5$ for the three-phase composite. Different periodic cell arrays are being considered: square array if the fundamental periods are $\omega_1 = 1$ and $\omega_2 = i$, hexagonal array if $\omega_1 = 1$ and $\omega_2 = e^{i\pi/3}$ and the general parallelogram array when fundamental periods $\omega_1 = 1$, $\omega_2 = e^{i\theta}$ and a vertex angle θ.

In Tables 2–5, the variation of the effective properties of MEE composites with different truncate orders **N** for a two- or three-phase composite are shown.

In Tables 2 and 3, some comparisons of the effective properties between the AHM, EEVM (Yan et al., 2013) and Kuo (2011) are shown for a three-phase composite (BaTiO₃/Terfenol-D/CoFe₂O₄) with square and hexagonal periodic cell respectively and a

Table 1
Magneto-electro-elastic materials properties.

	$C^{(\gamma)}_{55}$ (GPa)	$e^{(\gamma)}_{15}$ (C/m²)	$\kappa^{(\gamma)}_{11}$ (nF/m)	$q^{(\gamma)}_{15}$ (N/Am)	$\alpha^{(\gamma)}_{11}$ (10^{-12} Ns/VC)	$\mu^{(\gamma)}_{11}$ (10^{-6} N/A²)
BaTiO₃	43	11.6	11.2	0	0	5
CoFe₂O₄	45.3	0	0.08	550	0	590
Terfenol-D	13.6	0	0.05	108.3	0	5.4

Table 2
Variation of the effective MEE moduli obtained by AHM in term of order system **N**, for a three-phase composite with square periodic cell ($\theta = 90°$) and a comparison with those predicted EEVM (Yan et al., 2013) are shown.

BaTiO₃/Terfenol-D/CoFe₂O₄, $\lambda = V_2 + V_3 = 0.6$ $R_0/R = 4/5$											
N	C^*_{55} (GPa)		e^*_{15} (C/m²)		κ^*_{11} (nF/m)		q^*_{15} (N/Am)		μ^*_{11} (10^{-6} N/A²)		$-\alpha^*_{11}$ (10^{-12} Ns/VC)	
	AHM	EEVM	AHM	EEVM	AHM	EEVM	AHM	EEVM	AHM	EEVM	AHM	EEVM
1	37.04	37.14	0.05807	0.06011	0.1436	0.1466	176.4	206.1	141.6	178.8	60.73	67.59
3	37.04	37.05	0.05807	0.05821	0.1436	0.1438	176.2	178.4	141.2	144.0	60.59	61.28
5	37.04	37.04	0.05807	0.05807	0.1436	0.1436	176.2	176.3	141.2	141.4	60.59	60.63
7	37.04	37.04	0.05807	0.05807	0.1436	0.1436	176.2	176.2	141.3	141.3	60.59	60.59
9	37.04	37.04	0.05807	0.05807	0.1436	0.1436	176.2	176.2	141.3	141.2	60.59	60.59
Kuo	37.0		0.0599		0.147		175		140		63	

Table 3
The effective MEE moduli obtained by MHA in term of order system **N**, for a three-phase composite with hexagonal periodic cell ($\theta = 60°$) and a comparison with those predicted EEVM (Yan et al., 2013) and Kuo (2011) are shown.

BaTiO$_3$/Terfenol-D/CoFe$_2$O$_4$, $\lambda = V_2 + V_3 = 0.6$ $R_2/R_1 = 4/5$

N	C_{55}^* (GPa)		e_{15}^* (C/m^2)		κ_{11}^* (nF/m)		q_{15}^* (N/Am)		μ_{11}^* (10^{-6} N/A^2)		$-\alpha_{11}^*$ (10^{-12} Ns/VC)	
	AHM	EEVM	AHM	EEVM	AHM	EEVM	AHM	EEVM	AHM	EEVM	AHM	EEVM
1	37.05	37.07	0.05794	0.05838	0.1435	0.1441	184.8	191.2	152.4	160.4	63.81	64.67
3	37.05	37.05	0.05794	0.05794	0.1435	0.143	184	184	151.4	151.4	63.45	63.44
5	37.05	37.05	0.05794	0.05794	0.1435	0.143	184	184.1	151,4	151.4	63.45	63.46
7	37.05	37.05	0.05794	0.05794	0.1435	0.1435	184	184	151,4	151.4	63.45	63.45
9	37.05	37.05	0.05794	0.05794	0.1435	0.1435	184	184	151.4	151.4	63.45	63.45

Table 4
The effective MEE moduli obtained by AHM in term of order system **N** for a two-phase composite using the three-phase model.

BaTiO$_3$/CoFe$_2$O$_4$,

N	C_{55}^* (GPa)		e_{15}^* (C/m^2)		κ_{11}^* (nF/m)		q_{15}^* (N/Am)		μ_{11}^* (10^{-6} N/A^2)		$-\alpha_{11}^*$ (10^{-12} Ns/VC)	
	AHM	EEVM	AHM	EEVM	AHM	EEVM	AHM	EEVM	AHM	EEVM	AHM	EEVM
1	50.79	50.78	0.2579	0.2768	0.3362	0.3544	128.4	163.4	141.4	178.7	6.018	5.562
3	50.79	50.79	0.2588	0.2596	0.3371	0.3379	128.0	130.7	141.0	143.8	6.020	5.987
5	50.79	50.79	0.2588	0.2587	0.3371	0.337	128.0	128.1	141.0	141.1	6.020	6.019
7	50.79	50.79	0.2588	0.2588	0.3371	0.3371	128.0	128.0	141.0	141.0	6.020	6.020
9	50.79	50.79	0.2588	0.2588	0.3371	0.3371	128.0	128.0	141.0	141.0	6.020	6.020
Kuo	50.8		0.255		0.337		128		140		6.03	

good match between the approaches can be observed. In these comparisons, the volume fraction are considered to be $\lambda = V_2 + V_3 = 0.6$, $V_2 = (9/16)V_3$ because fibers radius relation is $R_2/R_1 = 4/5$ and $V_1 = 1 - V_2 - V_3$.

It can be noticed the influence of the arrangement of the cells on the properties of the composite and we can conclude that, for a three-phase composite materials (BaTiO$_3$/Terfenol-D/CoFe$_2$O$_4$), where the periodic cell is square, the magnetoelectric, magnetic, piezomagnetic and elastic properties are lower than those of the hexagonal cell, being opposite for the piezoelectric and dielectric properties. Also, it is observed that when the hexagonal fiber array is considered the results converge more rapidly than those for a square fiber array.

The effective properties of a bi-phase composite (BaTiO$_3$/CoFe$_2$O$_4$), can be derived from the three-phase model when the thickness of the interphase is very thin and the material properties are BaTiO$_3$ or CoFe$_2$O$_4$. In Table 4, the numerical results using the present model are compared with those reported by Yan et al. (2013) and Kuo (2011) when the periodic cell is square. Here, the volume fraction for each phase is considered as $\lambda = V_3 = 0.6$, $V_2 = 10^{-6}$ and $V_1 = 1 - V_2 - V_3$. It can be noticed that the result of the effective magnetoelectroelastic moduli is a good estimation. In addition, it was found that the interphase volume fraction has a strong influence on the effective properties because the results converge more rapidly when is considered the volume of the interphase as $V_2 < 10^{-6}$. The obtained values are closer to those reported by Yan et al. (2013).

An objective of making magnetoelectroelastic composites is to maximize the magnetoelectric coefficient. The highest one is obtained for the three-phase composite. This result is also obtained by Yan et al. (2013) even if Terfenol-D is considered instead of CoFe$_2$O$_4$. Then, the intermediate or interphase plays an important role in the mechanical interaction between the piezoelectric and magnetostrictive constituents leading to an extra improvement of the magnetoelectric coupling. In addition, for three-phase composites where the fibers are aligned with square periodicity, the magnetoelectric property is weaker than those of the composites with hexagonal or parallelogram periodicity, see Tables 2–4.

Table 5
The effective magnetoelectric (ME) moduli obtained by AHM in term of order system **N** for a three-phase composite (BaTiO$_3$/Terfenol-D/CoFe$_2$O$_4$) with Parallelogram periodic cell (($\theta = 75°$) and the fraction of volume of the interphase $V_3 = 0.6$.

Magnetoelectric coefficients (BaTiO$_3$/Terfenol-D/CoFe$_2$O$_4$)

N	$-\alpha_{11}^*$ (10^{-12} Ns/VC)		$-\alpha_{22}^*$ (10^{-12} Ns/VC)		$-\alpha_{12}^*$ (10^{-12} Ns/VC)	
	AHM	EEVM	AHM	EEVM	AHM	EEVM
1	68.75	70.82	54.39	63.98	0.1528	−1.996
3	68.60	68.74	53.23	55.63	0.1512	0.2091
5	68.60	68.60	53.18	53.70	0.1520	0.1971
7	68.60	68.60	53.18	53.32	0.1520	0.1793
9	68.60	68.60	53.18	53.30	0.1520	0.1780
11	68.60	68.60	53.18	53.17	0.1520	0.1511
13	68.60	68.60	53.18	53.18	0.1520	0.1520

In Table 5, a comparison of the magnetoelectric (ME) effective properties between the AHM and EEVM (Yan et al., 2013) is shown for a three-phase composite with parallelogram periodic cell and a good match between the approaches can be observed. Note that, new coefficients ME appears for this parallelogram periodic cell, i.e., the effective coefficients α_{12}^* and α_{21}^* are different of zero. For this case, it can be observed the influence of the cell's space fiber distribution on the anisotropic symmetry.

Therefore, the overall magnetoelectric performance of the composite with parallelogram periodic cell has less symmetry operations than hexagonal and square periodic cell, which exhibit a transversely isotropic symmetry as was reported by the previous work, Camacho-Montes et al. (2009), Espinosa-Almeyda et al. (2011), Kuo (2011) and Kuo and Pan (2011) for a square periodic cell and Espinosa-Almeyda et al. (2011) and Yan et al. (2013) for a hexagonal periodic cell. In both types of cells, ME effective coefficients satisfy that $\alpha_{12}^* = \alpha_{21}^* = 0$ and $\alpha_{11}^* = \alpha_{22}^* \neq 0$. When the periodic cell is represented by parallelogram $\alpha_{12}^* = \alpha_{21}^* \neq 0$ and $\alpha_{11}^* \neq \alpha_{22}^*$. For this last case, it is also possible to observe that the following effective properties are no null: $C_{55}^* \neq C_{44}^*$, $e_{15}^* \neq e_{24}^*$, $q_{15}^* \neq q_{24}^*$, $\kappa_{11}^* \neq \kappa_{22}^*$, $\mu_{11}^* \neq \mu_{22}^*$ and $C_{45}^* = C_{54}^*$, $e_{25}^* = e_{14}^*$, $q_{25}^* = q_{14}^*$, $\kappa_{12}^* = \kappa_{21}^*$, $\mu_{12}^* = \mu_{21}^*$. Consequently, the composite with parallelogram cell corresponds to a material behavior with a higher

Table 6
Variation of the effective MEE moduli obtained by MHA in term of order system N and volume fractions $\lambda = 0.2$ and $\lambda = 0.85$, for an idealized three-phase composite (BaTiO$_3$/Terfenol-D/CoFe$_2$O$_4$) with hexagonal periodic cell and the contrast between the fiber and matrix is 120.

(BaTiO$_3$/Terfenol $-$ D/CoFe$_2$O$_4$) $V_2 = (1/16)V_3$, $V_1 = 1 - V_2 - V_3$							
V_3	N	C_{55}^* (GPa)	e_{15}^* (C/m^2)	κ_{11}^* (nF/m)	q_{15}^* (N/Am)	$-\alpha_{11}^*$ (10^{-12} Ns/VC)	μ_{11}^* (10^{-6} N/A^2)
0.2	1	64.246	0.0006	0.1182	594.59	4.2563	457.73
	2	64.246	0.0006	0.1182	594.59	4.2563	457.73
	7	64.246	0.0006	0.1182	594.59	4.2563	457.73
0.85	1	293.83	0.0368	0.8065	1778.7	220.67	170.88
	7	304.62	0.0456	0.9248	1826.5	271.02	162.25
	10	304.62	0.0456	0.9248	1826.2	271.00	162.06
	15	304.62	0.0456	0.9248	1826.1	270.99	161.99
	16	304.62	0.0456	0.9248	1826.1	270.90	161.98

anisotropic degree, as it was pointed out previously. For these fibrous composites, the maximum value tolerable of the fiber volume fraction λ is 0.785 for a square cell, 0.906 for a hexagonal cell and 0.813 for parallelogram periodic cell with angle of 75° and 1 for an idealized even fiber distribution in the Mori–Tanaka estimation (Wang and Pan, 2007), consequently with the results of Yan et al. (2013).

We assert from comparisons in Tables 2–5 that both methods AHM and EEVM are in a good concordance except the effective properties q_{15}^*, μ_{11}^* and α_{11}^* for only N = 1. Also, we analyze the behavior of the analytical expression using N = 1 (short formulae see (23)) whose numerical computations are shown in the aforementioned tables.

As it was mentioned previously, the solution to the infinite order algebraic system (22) is achieved by means of truncation to an infinite order and the Gauss's method. A fast convergence of successive truncations is ensured because the system is regular (Rodríguez-Ramos et al. (2001)) so that successive approximations can be applied. Besides, concerning the well convergence of the AHM we can refer to Sixto-Camacho et al. (2013) and Bravo-Castillero et al. (2008).

In general, for the volume fraction of each phase, as it is considered in Table 4 where $\lambda = V_3 = 0.6$, (Fiber) $V_2 \leqslant 10^{-6}$ (interphase) and $V_1 = 1 - V_2 - V_3$ (matrix), the accuracy and convergence of the results are good for smaller values of N ($N \leqslant 3$). More terms are required to be included for high volume fraction of fibers as well as for higher contrast between the fiber and matrix as it can be observed in the next example.

An analysis of computational cost required to achieve pre-fixed accuracy as a function of volume fraction $\lambda = V_2 + V_3$ and material properties is shown in Table 6. Here, the effective properties obtained by MHA are computed for a three-phase composite with a BaTiO$_3$ matrix, Terfenol-D interphase and idealized properties of fiber. This combination is proposed to obtain a higher contrast between the matrix and fiber. In this example, we used the fiber properties of CoFe$_2$O$_4$ multiplied by 120 with hexagonal periodic cell ($\theta = 60°$) for two different volume fractions $V_3 = 0.2$ and $V_3 = 0.85$ (case close to percolation), $V_2 = (1/16)V_3$ and $V_1 = 1 - V_2 - V_3$.

It can be noticed from Table 6 that good accuracy is already reached for low values of N for effective magnetoelectroelastic properties when the fiber volume fraction ($\lambda = 0.2125$) is small, i.e., $N \leqslant 2$. For high fiber volume fraction ($\lambda = 0.9031$), it is needed a higher truncation order N of equation systems (21) to get a better accuracy. The solution (22) depends on powers of radius R_1 (see in (18) expression of w_{kp}), then more terms are required to assure the convergence of the solution, for higher volume fraction. In addition, it is worthily to mention that computation of the result only takes few seconds.

Fig. 2 illustrates the behavior of the effective magnetoelectric coefficient α_{11}^* calculated by AHM, for two-phase composite
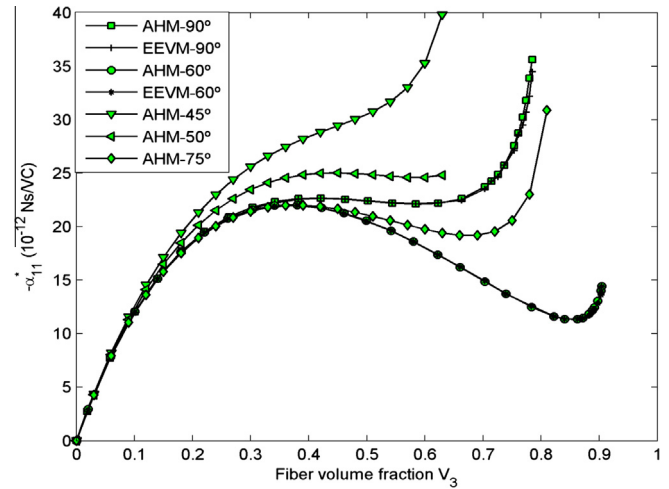
Fig. 2. Effective magnetoelectric coefficient α_{11}^* for the two-phase composites (Terfenol-D/BaTiO$_3$) for different periodic cells versus the fiber volume fraction. A comparison of the present model with EEVM approach (Yan et al., 2013), for square and hexagonal fiber array are illustrated.

Terfenol-D/BaTiO$_3$ with parallelogram periodic cell versus the fiber volume fraction V_3, up to the percolation limit. The volume fraction of the interphase is $V_2 = 10^{-6}$. The numerical results derived by AHM are compared with EEVM method (see Yan et al., 2013) for square and hexagonal cells. Very close results can be seen between the two models.

The effective properties of the composites shown in Fig 2 are transversely isotropic at the angles 60° (hexagonal periodic cell) and 90° (square periodic cell), the strongest anisotropy appear at angle 45°. In the range between 60° and 90° the trend of the curves of all coefficients are similar, being different for high fiber volume fraction values. The difference between the coefficients is remarkable for angles of the cell less than 60°. The explanation should be given because of the fact that in the distance between the fibers is small and it reinforces the properties of the composite in this direction.

Also, from Fig. 2, it is possible to see that, for small fiber volume fraction, this type of the cell distribution does not affect the value of the effective property; it is the same value in both distributions (square and hexagonal distribution cell). However, when the Terfenol $-$ D fiber volume fraction is growing, the fiber distribution show to have a heavier role on the ME coefficients. When the fibers are aligned with hexagonal distribution the property α_{11}^* is weaker than square distribution properties. We can also see, that the property α_{11}^* reaches local extreme maximum and minimum values, and finally increases rapidly until the fiber volume fraction reach the percolation limit.
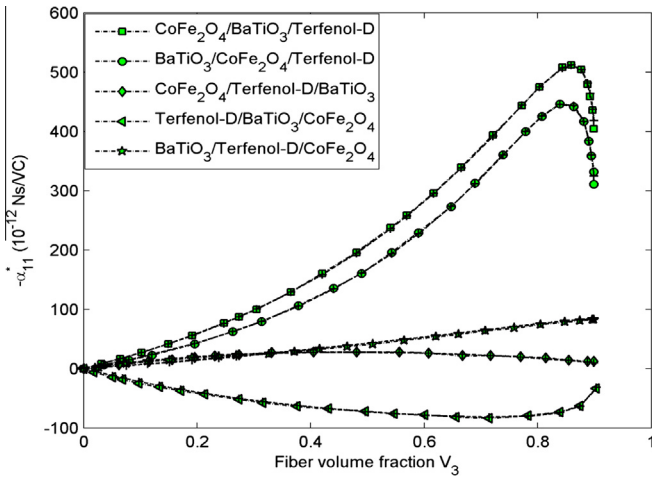
Fig. 3. Effective magnetoelectric coefficient α_{11}^* of the different three-phase composites versus the total volume fraction of the fiber and interphase for a hexagonal fiber array.
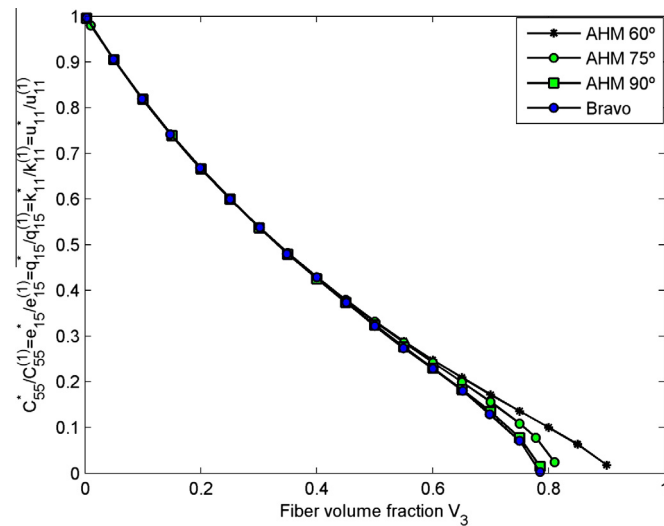

Fig. 4. The normalized effective properties of the three-phase composite with empty fibers versus the total volume fraction of the fiber and interphase for different fiber array.

Table 7
Piezoelectric materials properties.

	BaTiO$_3$	Hollow	Epoxy	Glass	PZT
$C_{55}^{(\gamma)}$ (GPa)	43.86	0	1.8	29.6	25.696
$e_{15}^{(\gamma)}$ (C/m^2)	11.4	0	0	0	9.35
$\kappa_{11}^{(\gamma)}$ (nF/m)	12.8	0.00886	0.0372	0.0566	4.065

The first maximum for the ME coupling has been previously reported by Camacho-Montes et al. (2009) and Espinosa-Almeyda et al. (2011). The ME coupling in the type of composite studied herein, where there is no ME effect for either of the constituents is a result of the mechanical interaction at the interphase between piezoelectric and piezomagnetic constituents. In principle, the first maximum can be expected for $V_3 = 0.5$. However, depending on the constituent properties this maximum can shift either to higher or lower matrix volume fraction. It is worthily to observe that a second tendency of the ME to increase toward fiber percolations. This interesting fact is probably related to the interceptions of the stress field of different matrix-fiber interphases as they are closer near percolation. This effect can also be related to the presence of the interphase as it is not observed by Camacho-Montes et al. (2009).

In Fig. 3, the effective Magnetoelectric coefficient α_{11}^* of the three-phase composite $((R_2/R_1)^2 = 1/2 \Longleftrightarrow V_2 = V_3)$ versus the total volume fraction of the fiber and interphase $\lambda = V_2 + V_3$, up to the percolation limit for hexagonal periodic cell are shown. A comparison for the present solutions by AHM with those predicted by EEVM (Yan et al., 2013) for different kinds of three-phase composites composed of CoFe$_2$O$_4$, BaTiO$_3$ and Terfenol-D in different permutations is also performed. Note that, good estimations can be reported. We can verify that the biggest value for α_{11}^* is -512.2×10^{-12}Ns/VC for CoFe$_2$O$_4$/BaTiO$_3$/Terfenol-D composite when the fiber volume fraction is 0.86 as it is reported by Yan et al. (2013). It is important to note, besides the choice of the phases, the influence of the permutation can also be significant in the behavior of the new effective coefficient.

The effect of the shape of the cross-section of the empty fibers obtained by AHM method for a three-phase composite (Empty/Empty/BaTiO$_3$) are shown here to illustrate the effect of the empty-fibers cross-section shape on the antiplane properties C_{55}^*, e_{15}^*, q_{15}^*, κ_{11}^* and μ_{11}^*, see Fig 4. The AHM-90° curve shows total coincidence with the results reported by Bravo-Castillero et al. (2009) for BaTiO$_3$ porous material.

The Fig 4 shows that the universal relations $C_{55}^*/C_{55}^{(1)} = e_{15}^*/e_{15}^{(1)} = q_{15}^*/q_{15}^{(1)} = \kappa_{11}^*/\kappa_{11}^{(1)} = \mu_{11}^*/\mu_{11}^{(1)}$ are satisfied for a porous fiber composite. It can also be observed, from this figure, that the curves do not cross each other and that the ratios decrease monotonically from the matrix value (normalized to 1) at zero fiber volume fraction to the corresponding percolation limit. In addition, very closed estimation between the curves for small values of the fiber volume fraction are observed. The equalities shown previously are published by Bravo-Castillero et al. (2009) for 1-3 piezoelectric composites and they are extended for MEE composites in formula (3.59) in Bravo-Castillero et al. (2012),

7.1. Piezoelectric composites

The effective coefficients (26) and (27) can be reduced to piezoelectric, bi- or three-phase composites. These effective properties are compared with those published by Yan et al.

Table 8
The effective piezoelectric moduli in term of order system **N** for a three-phase composite with square periodic cell.

	Glass/PZT/Epoxy, (Square cell)						Glass/PZT/Epoxy, (Hexagonal cell)					
N	C_{55}^* (GPa)		e_{15}^* (C/m^2)		κ_{11}^* (nF/m)		C_{55}^* (GPa)		e_{15}^* (C/m^2)		κ_{11}^* (nF/m)	
	AHM	EEVM	AHM	EEVM	AHM	EEVM	AHM	EEVM	AHM	EEVM	AHM	EEVM
1	6.452	6.755	0.0562	0.0613	0.1488	0.1563	6.116	6.231	0.0461	0.0486	0.1390	0.1420
3	6.462	6.477	0.0566	0.0568	0.1492	0.1495	6.144	6.141	0.0468	0.0468	0.1398	0.1397
5	6.462	6.462	0.0566	0.0566	0.1492	0.1492	6.144	6.144	0.0468	0.0468	0.1398	0.1398
7	6.462	6.462	0.0566	0.0566	0.1492	0.1492	6.144	6.144	0.0468	0.0468	0.1398	0.1398
9	6.462	6.462	0.0566	0.0566	0.1492	0.1492	6.144	6.144	0.0468	0.0468	0.1398	0.1398

(2011) by EEVM for different fibers arrays and different fibers volume fraction. It will be shown in Table 8. In these cases, the material properties are considered in the following Table 7; see Yan et al. (2011).

In Table 8, the effective properties of a three-phase piezoelectric composite (Glass/PZT/Epoxy), with square or hexagonal periodic cell obtained by AHM are summarized, and compared with those reported by EEVM (Yan et al., 2011). Here, the volume total of the fiber (Glass) and interphase (PZT) is $\lambda = V_2 + V_3 = 0.6$, the relative radius of the fibers are given as $R_0/R = 2/3$ and the fraction of volume of the phases are $V_2 = (5/4) \cdot V_3$ and $V_1 = 1 - V_2 - V_3$. From Table 8, a good agreement and rapid convergence of the present results are observed.

8. Conclusions

In this work, the analytical formulae derived for all effective properties have a simple form. The computational implementation is easy. In addition to its theoretical importance, they can be used for checking the implementation of experimental, numerical and analytical models. The numerical analysis demonstrates that the AHM model is very simple, accurate and efficient for the analysis of fiber-reinforced composites with presence of the interphase and for different arrangement of angular distribution of the fibers. In addition, is remarkable the relation among the contrasts of the phases properties, the order of truncation and the volume fractions of the fiber and the interphase. Some comparisons with experimental results reported in the literature revealed a good performance. The formulae are also valid for two- or three-phase piezoelectric or elastic composite. For composites with a parallelogram periodic array of fibers, the effective magnetoelectric moduli can be anisotropic. There exist two new coupling magnetoelectric coefficients besides the two main coefficients.

Appendix A

The local problems are transformed into dimensionless problems, making the following transformations (Wang and Ding, 2006).

$$E_{\beta 5}^{(\gamma)} \sqrt{C_{\beta 3\beta 3}^{(\gamma)} \kappa_{\beta\beta}^{(\gamma)}} = e_{\beta\beta 3}^{(\gamma)}, \quad Q_{\beta 5}^{(\gamma)} \sqrt{C_{\beta 3\beta 3}^{(\gamma)} \mu_{\beta\beta}^{(\gamma)}} = q_{\beta\beta 3}^{(\gamma)}, \quad A_{\beta\beta}^{(\gamma)} \sqrt{\kappa_{\beta\beta}^{(\gamma)} \mu_{\beta\beta}^{(\gamma)}} = \alpha_{\beta\beta}^{(\gamma)},$$

$$\mu^{(s)*} = \mu_{\alpha\alpha}^{(s+1)}/\mu_{\alpha\alpha}^{(1)}, \quad C_{1313}^{(\gamma)} \tilde{\sigma}_{i3}^{(\gamma)} = \sigma_{i3}^{(\gamma)}, \quad C_{1313}^{(\gamma)} \kappa_{11}^{(\gamma)} \tilde{D}_{i3}^{(\gamma)} = D_{i3}^{(\gamma)},$$

$$C_{1313}^{(\gamma)} \mu_{11}^{(\gamma)} \tilde{B}_{i3}^{(\gamma)} = B_{i3}^{(\gamma)},$$

$$l\mathcal{L}_3^{(\gamma)} = \tilde{\mathcal{L}}_3^{(\gamma)}, \quad l\mathcal{M}^{(\gamma)} = \sqrt{\kappa_{11}^{(\gamma)}/C_{1313}^{(\gamma)}} \tilde{\mathcal{M}}^{(\gamma)}, \quad l\mathcal{N}^{(\gamma)} = \sqrt{\mu_{11}^{(\gamma)}/C_{1313}^{(\gamma)}} \tilde{\mathcal{N}}^{(\gamma)},$$

$$\kappa^{(s)*} = \kappa_{\alpha\alpha}^{(s+1)}/\kappa_{\alpha\alpha}^{(1)}$$

$$l\mathcal{P}_3^{(\gamma)} = \sqrt{C_{1313}^{(\gamma)}/\kappa_{11}^{(\gamma)}} \tilde{\mathcal{P}}_3^{(\gamma)}, \quad l\mathcal{Q}^{(\gamma)} = \tilde{\mathcal{Q}}^{(\gamma)}, \quad l\mathcal{R}^{(\gamma)} = \sqrt{\mu_{11}^{(\gamma)}/\kappa_{11}^{(\gamma)}} \tilde{\mathcal{R}}^{(\gamma)},$$

$$\chi^{(s)*} = C_{\beta 3\beta 3}^{(s+1)}/C_{\beta 3\beta 3}^{(1)}$$

$$l\sqrt{\mu_{11}^{(\gamma)}/C_{1313}^{(\gamma)}} \mathcal{S}_3^{(\gamma)} = \tilde{\mathcal{S}}_3^{(\gamma)}, \quad l\sqrt{\mu_{11}^{(\gamma)}/\kappa_{11}^{(\gamma)}} \mathcal{T}^{(\gamma)} = \tilde{\mathcal{T}}^{(\gamma)},$$

$$l\mathcal{V}^{(\gamma)} = \tilde{\mathcal{V}}^{(\gamma)}, \quad lR = R_0, \quad l\xi = \mathbf{y}.$$

Appendix B

In order to realize the numerical calculations we present the following algorithm which allows us to derive the system (21). The relations defined in Wang and Ding (2006) (Appendix A) are used, substituting the previous expansion (18)–(20) into contact conditions (14) for $s = 1, 2$ and considering that $z = R_s e^{i\theta}$ for different powers of $e^{ip\theta}$ we obtain the following equations:

$$\left[a_0 \delta_{1p} + \sum_{k=1}^{\infty}{}^o a_k \eta_{kp} + \bar{a}_p \right] R_2^p = a_p^{(2)} R_1^p + \bar{a}_{-p}^{(2)} R_2^p$$

$$\left[b_0 \delta_{1p} + \sum_{k=1}^{\infty}{}^o b_k \eta_{kp} + \bar{b}_p \right] R_2^p = \sqrt{\chi^{(1)*}/\kappa^{(1)*}}(b_p^{(2)} R_1^p + \bar{b}_{-p}^{(2)} R_2^p), \quad \text{on} \quad \Gamma_1$$

$$\left[e_0 \delta_{1p} + \sum_{k=1}^{\infty}{}^o e_k \eta_{kp} + \bar{e}_p \right] R_2^p = \sqrt{\chi^{(1)*}/\mu^{(1)*}}(e_p^{(2)} R_1^p + \bar{e}_{-p}^{(2)} R_2^p),$$

$$\text{(B.1)}$$

$$a_p^{(2)} R_2^p + \bar{a}_{-p}^{(2)} R_1^p = c_p R_2^p,$$

$$\sqrt{\chi^{(1)*} \kappa^{(2)*}} \left[b_p^{(2)} R_2^p + \bar{b}_{-p}^{(2)} R_1^p \right] = \sqrt{\kappa^{(1)*} \chi^{(2)*}} d_p R_2^p, \quad \text{on} \quad \Gamma_2 \qquad \text{(B.2)}$$

$$\sqrt{\chi^{(1)*} \mu^{(2)*}} \left[e_p^{(2)} R_2^p + \bar{e}_{-p}^{(2)} R_1^p \right] = \sqrt{\mu^{(1)*} \chi^{(2)*}} f_p R_2^p.$$

Now, the local functions are considered periodic harmonic functions of the complex variable and they satisfy the Cauchy-Riemann conditions, using the relations defined in Appendix A, $[\![f_i]\!] = f_i(z) - \bar{f}_i(z)$ and $n_2 = -R^{-1}(dx_1/d\theta)$, $n_1 = R^{-1}(dx_2/d\theta)$ on the interfaces Γ_s, the equalities (15) can be written in terms of the complex functions as:

$$\left[\begin{matrix} [\![f_1]\!] + E_{15}^{(1)}[\![g_1]\!] + Q_{15}^{(1)}[\![h_1]\!] + (1 - \chi^{(1)*})\delta_{\alpha 1}(z - \bar{z}) \\ = \chi^{(1)*} \left[[\![f_2]\!] + E_{15}^{(2)}[\![g_2]\!] + Q_{15}^{(2)}[\![h_2]\!] \right] + (1 - \chi^{(1)*})i\delta_{\alpha 2}(z + \bar{z}) \end{matrix} \right]_{\Gamma_1}$$

$$\left[\begin{matrix} \chi^{(1)*}[\![f_2]\!] + E_{15}^{(2)}[\![g_2]\!] + Q_{15}^{(2)}[\![h_2]\!]] + (\chi^{(2)*} - \chi^{(1)*})i\delta_{\alpha 2}(z + \bar{z}) \\ = (\chi^{(2)*} - \chi^{(1)*})\delta_{\alpha 1}(z - \bar{z}) + \chi^{(2)*} \left[[\![f_3]\!] + E_{15}^{(3)}[\![g_3]\!] + Q_{15}^{(3)}[\![h_3]\!] \right] \end{matrix} \right]_{\Gamma_2}$$

$$\text{(B.3)}$$

$$\left[\begin{matrix} E_{15}^{(1)}[\![f_1]\!] - [\![g_1]\!] - A_{11}^{(1)}[\![h_1]\!] + \left(E_{15}^{(1)} - \sqrt{\chi^{(1)*}\kappa^{(1)*}}E_{15}^{(2)} \right)(z - \bar{z})\delta_{\alpha 1} \\ = \sqrt{\chi^{(1)*}\kappa^{(1)*}} \left[E_{15}^{(2)}[\![f_2]\!] - [\![g_2]\!] - A_{11}^{(2)}[\![h_2]\!] \right] + i\left(E_{15}^{(1)} - \sqrt{\chi^{(1)*}\kappa^{(1)*}}E_{15}^{(2)} \right)(z + \bar{z})\delta_{\alpha 2} \end{matrix} \right]_{\Gamma_1}$$

$$\left[\begin{matrix} \sqrt{\chi^{(1)*}\kappa^{(1)*}} \left[E_{15}^{(2)}[\![f_2]\!] - [\![g_2]\!] - A_{11}^{(2)}[\![h_2]\!] \right] + \left(\sqrt{\chi^{(1)*}\kappa^{(1)*}}E_{15}^{(2)} - \sqrt{\chi^{(2)*}\kappa^{(2)*}}E_{15}^{(3)} \right)(z - \bar{z})\delta_{\alpha 1} \\ = \sqrt{\chi^{(2)*}\kappa^{(2)*}} \left[E_{15}^{(3)}[\![f_3]\!] - [\![g_2]\!] - A_{11}^{(3)}[\![h_3]\!] \right] + i\left(\sqrt{\chi^{(1)*}\kappa^{(1)*}}E_{15}^{(2)} - \sqrt{\chi^{(2)*}\kappa^{(2)*}}E_{15}^{(3)} \right)\delta_{\alpha 2}(z + \bar{z}) \end{matrix} \right]_{\Gamma_2}$$

$$\text{(B.4)}$$

$$\left[\begin{matrix} Q_{15}^{(1)}(\delta_{\alpha 1}(z - \bar{z}) - i\delta_{\alpha 2}(z + \bar{z})) + Q_{15}^{(1)}[\![f_1]\!] - A_{11}^{(1)}[\![g_1]\!] - [\![h_1]\!] \\ = Q_{15}^{(2)}(\delta_{\alpha 1}(z - \bar{z}) - i\delta_{\alpha 2}(z + \bar{z})) + \sqrt{\chi^{(1)*}\mu^{(1)*}} \left[Q_{15}^{(2)}[\![f_2]\!] - A_{11}^{(2)}[\![g_2]\!] - [\![h_2]\!] \right] \end{matrix} \right]_{\Gamma_1}$$

$$\left[\begin{matrix} \sqrt{\chi^{(1)*}\mu^{(1)*}} \left[Q_{15}^{(2)}(\delta_{\alpha 1}(z - \bar{z}) - i\delta_{\alpha 2}(z + \bar{z})) + Q_{15}^{(2)}[\![f_2]\!] - A_{11}^{(2)}[\![g_2]\!] - [\![h_2]\!] \right] \\ = \sqrt{\chi^{(2)*}\mu^{(2)*}} \left[Q_{15}^{(3)}(\delta_{\alpha 1}(z - \bar{z}) - \delta_{\alpha 2}(z + \bar{z})) + Q_{15}^{(3)}[\![f_3]\!] - A_{11}^{(3)}[\![g_3]\!] - [\![h_3]\!] \right] \end{matrix} \right]_{\Gamma_2}$$

$$\text{(B.5)}$$

Then substituting the expansion (18)–(20) into the previous equations (B.3)–(B.5) at the interface Γ_s and analogous to the way for obtaining (B.1) and (B.2), the following equations characterize the contact conditions.

$$\left\{\left[a_0\delta_{1p}+\sum_{k=1}^{\infty}{}^o a_k\eta_{kp}-\bar{a}_p\right]+E_{15}^{(1)}\left[b_0\delta_{1p}+\sum_{k=1}^{\infty}{}^o b_k\eta_{kp}-\bar{b}_p\right]+Q_{15}^{(1)}\left[e_0\delta_{1p}+\sum_{k=1}^{\infty}{}^o e_k\eta_{kp}-\bar{e}_p\right]\right\}R_2^p$$
$$=\chi^{(1)*}\left\{\left[a_p^{(2)}+E_{15}^{(2)}b_p^{(2)}+Q_{15}^{(2)}e_p^{(2)}\right]R_1^p-\left[\bar{a}_{-p}^{(2)}+E_{15}^{(2)}\bar{b}_{-p}^{(2)}+Q_{15}^{(2)}\bar{e}_{-p}^{(2)}\right]R_2^p\right\}-(1-\chi^{(1)*})R_2^pR_1[\delta_{\alpha1}-i\delta_{\alpha2}]\delta_{1p},$$
$$\chi^{(1)*}\left\{\left[a_p^{(2)}+E_{15}^{(2)}b_p^{(2)}+Q_{15}^{(2)}e_p^{(2)}\right]R_2^p-\left[\bar{a}_{-p}^{(2)}+E_{15}^{(2)}\bar{b}_{-p}^{(2)}+Q_{15}^{(2)}\bar{e}_{-p}^{(2)}\right]R_1^p\right\}=\chi^{(2)*}\left[c_p+E_{15}^{(3)}d_p+Q_{15}^{(3)}f_p\right]R_2^p+(\chi^{(2)*}-\chi^{(1)*})R_2^{p+1}[\delta_{\alpha1}-i\delta_{\alpha2}]\delta_{1p},$$

(B.6)

$$\left\{E_{15}^{(1)}\left[a_0\delta_{1p}+\sum_{k=1}^{\infty}{}^o a_k\eta_{kp}-\bar{a}_p\right]-\left[b_0\delta_{1p}+\sum_{k=1}^{\infty}{}^o b_k\eta_{kp}-\bar{b}_p\right]-A_{11}^{(1)}\left[e_0\delta_{1p}+\sum_{k=1}^{\infty}{}^o e_k\eta_{kp}-\bar{e}_p\right]\right\}R_2^p$$
$$=\sqrt{\chi^{(1)*}\kappa^{(1)*}}\left\{\left[E_{15}^{(2)}a_p^{(2)}-A_{11}^{(2)}e_p^{(2)}-b_p^{(2)}\right]R_1^p-\left[E_{15}^{(2)}\bar{a}_{-p}^{(2)}-A_{11}^{(2)}\bar{e}_{-p}^{(2)}-\bar{b}_{-p}^{(2)}\right]R_2^p\right\}-\left(E_{15}^{(1)}-\sqrt{\chi^{(1)*}\kappa^{(1)*}}E_{15}^{(2)}\right)R_2^pR_1\delta_{1p}[\delta_{\alpha1}-i\delta_{\alpha2}],$$
$$\sqrt{\chi^{(1)*}\kappa^{(1)*}}\left\{\left[E_{15}^{(2)}a_p^{(2)}-b_p^{(2)}-A_{11}^{(2)}e_p^{(2)}\right]R_2^p-\left[E_{15}^{(2)}\bar{a}_{-p}^{(2)}-\bar{b}_{-p}^{(2)}-A_{11}^{(2)}\bar{e}_{-p}^{(2)}\right]R_1^p\right\}$$
$$=\sqrt{\chi^{(2)*}\kappa^{(2)*}}\left[E_{15}^{(3)}c_p-d_p-A_{11}^{(3)}f_p\right]R_2^p-\left(\sqrt{\chi^{(1)*}\kappa^{(1)*}}E_{15}^{(2)}-\sqrt{\chi^{(2)*}\kappa^{(2)*}}E_{15}^{(3)}\right)R_2^{p+1}\delta_{1p}[\delta_{\alpha1}-i\delta_{\alpha2}],$$

(B.7)

$$\left\{Q_{15}^{(1)}\left[a_0\delta_{1p}+\sum_{k=1}^{\infty}{}^o a_k\eta_{kp}-\bar{a}_p\right]-A_{11}^{(1)}\left[b_0\delta_{1p}+\sum_{k=1}^{\infty}{}^o b_k\eta_{kp}-\bar{b}_p\right]-\left[e_0\delta_{1p}+\sum_{k=1}^{\infty}{}^o e_k\eta_{kp}-\bar{e}_p\right]\right\}R_2^p$$
$$=\sqrt{\chi^{(1)*}\mu^{(1)*}}\left\{\left[Q_{15}^{(2)}a_p^{(2)}-e_p^{(2)}-A_{11}^{(2)}b_p^{(2)}\right]R_1^p-\left[Q_{15}^{(2)}\bar{a}_{-p}^{(2)}-\bar{e}_{-p}^{(2)}-A_{11}^{(2)}\bar{b}_{-p}^{(2)}\right]R_2^p\right\}-\left(Q_{15}^{(1)}-\sqrt{\chi^{(1)*}\mu^{(1)*}}Q_{15}^{(2)}\right)R_2^pR_1\delta_{1p}[\delta_{\alpha1}-i\delta_{\alpha2}],$$
$$\sqrt{\chi^{(1)*}\mu^{(1)*}}\left\{\left[Q_{15}^{(2)}a_p^{(2)}-A_{11}^{(2)}b_p^{(2)}-e_p^{(2)}\right]R_2^p-\left[Q_{15}^{(2)}\bar{a}_{-p}^{(2)}-A_{11}^{(2)}\bar{b}_{-p}^{(2)}-\bar{e}_{-p}^{(2)}\right]R_1^p\right\}$$
$$=\sqrt{\chi^{(2)*}\mu^{(2)*}}\left[Q_{15}^{(3)}c_p-A_{11}^{(3)}d_p-f_p\right]R_2^p-\left(\sqrt{\chi^{(1)*}\mu^{(1)*}}Q_{15}^{(2)}-\sqrt{\chi^{(2)*}\mu^{(2)*}}Q_{15}^{(3)}\right)R_2^{p+1}\delta_{1p}[\delta_{\alpha1}-i\delta_{\alpha2}],$$

(B.8)

We have obtained a system (B.1), (B.2) and (B.6)–(B.8) of twelve equations with the unknown constants $\bar{a}_p$, $a_p^{(2)}$, $\bar{a}_{-p}^{(2)}$, $\bar{b}_p$, $b_p^{(2)}$, $\bar{b}_{-p}^{(2)}$, $\bar{e}_p$, $e_p^{(2)}$, $\bar{e}_{-p}^{(2)}$, c_p, d_p and f_p. This system can be rewritten into a new matricial system (21) in term of the conjugate of $\bar{a}_p$, $\bar{b}_p$ and $\bar{e}_p$, which can be solved by Gauss's method. Once we have the unknown constants, we can determine the effective coefficients (24) and (25). The magnitudes that appear in system (21) corresponding to the local problem $_{\alpha3}\mathcal{L}$ can be summarized as follows:

$$\mathcal{A}_{\tau p}=(-1)^{\tau+1}+A_{(1)p}D_{(5)p}+A_{(3)p}D_{(8)p}+A_{(5)p}D_{(11)p},$$
$$\mathcal{B}_{\tau p}=(-1)^{\tau+1}E_{15}^{(1)}+A_{(1)p}D_{(6)p}+A_{(5)p}D_{(12)p}+A_{(3)p}D_{(9)p},\quad \tau=1,2,$$
$$\mathcal{C}_{\tau p}=(-1)^{\tau+1}Q_{15}^{(1)}+A_{(1)p}D_{(7)p}+A_{(5)p}D_{(13)p}+A_{(3)p}D_{(10)p},$$

$$\mathcal{A}_{\bar{\tau} p}=(-1)^{\bar{\tau}+1}E_{15}^{(1)}+B_{(1)p}D_{(5)p}-B_{(3)p}D_{(8)p}-B_{(5)p}D_{(11)p},$$
$$\mathcal{B}_{\bar{\tau} p}=(-1)^{\bar{\tau}}+B_{(1)p}D_{(6)p}-B_{(3)p}D_{(9)p}-B_{(5)p}D_{(12)p},\quad \bar{\tau}=3,4,$$
$$\mathcal{C}_{\bar{\tau} p}=(-1)^{\bar{\tau}}A_{11}^{(1)}+B_{(1)p}D_{(7)p}-B_{(3)p}D_{(10)p}-B_{(5)p}D_{(13)p},$$

$$\mathcal{A}_{\tilde{\tau} p}=(-1)^{\tilde{\tau}+1}Q_{15}^{(1)}+C_{(1)p}D_{(5)p}-C_{(3)p}D_{(8)p}-C_{(5)p}D_{(11)p},$$
$$\mathcal{B}_{\tilde{\tau} p}=(-1)^{\tilde{\tau}}A_{11}^{(1)}+C_{(1)p}D_{(6)p}-C_{(3)p}D_{(9)p}-C_{(5)p}D_{(12)p},\quad \tilde{\tau}=5,6,$$
$$\mathcal{C}_{\tilde{\tau} p}=(-1)^{\tilde{\tau}}+C_{(1)p}D_{(7)p}-C_{(3)p}D_{(10)p}-C_{(5)p}D_{(13)p},$$

the independent term for the local problem $_{\alpha3}\mathscr{L}$ are

$$\mathcal{T}_{1p}=\left(1-\chi^{(1)*}\right)R_1+(\chi^{(1)*}-\chi^{(2)*})\mathscr{E}_p^+R_2$$
$$-\left(A_{(1)p}G_{(3)p}+A_{(3)p}G_{(4)p}+A_{(5)p}G_{(5)p}\right)\mathscr{E}_p^-R_2,$$

$$\mathcal{T}_{2p}=\left(E_{15}^{(1)}-E_{15}^{(2)}\sqrt{\chi^{(1)*}\kappa^{(1)*}}\right)R_1$$
$$+\left[\left(E_{15}^{(2)}\sqrt{\chi^{(1)*}\kappa^{(1)*}}-E_{15}^{(3)}\sqrt{\chi^{(2)*}\kappa^{(2)*}}\right)\mathcal{E}_p^+\right.$$
$$\left.-\left(B_{(1)p}G_{(3)p}-B_{(3)p}G_{(4)p}-B_{(5)p}G_{(5)p}\right)\mathcal{E}_p^-\right]R_2,$$

$$\mathcal{T}_{3p}=\left(Q_{15}^{(1)}-Q_{15}^{(2)}\sqrt{\chi^{(1)*}\mu^{(1)*}}\right)R_1$$
$$+\left[\left(Q_{15}^{(2)}\sqrt{\chi^{(1)*}\mu^{(1)*}}-Q_{15}^{(3)}\sqrt{\chi^{(2)*}\mu^{(2)*}}\right)\mathcal{E}_p^+\right.$$
$$\left.-\left(C_{(1)p}G_{(3)p}-C_{(3)p}G_{(4)p}-C_{(5)p}G_{(5)p}\right)\mathcal{E}_p^-\right]R_2,$$

with,

$$A_{(\tau)p}=\frac{1}{2}\left[\left(\chi^{(1)*}+\chi^{(2)*}\right)\mathscr{d}_p+(-1)^\tau\left(\chi^{(1)*}-\chi^{(2)*}\right)\mathscr{d}_p^{-1}\right],$$

$$B_{(\tau)p}=\frac{1}{2}\left[\left(E_{15}^{(2)}\sqrt{\chi^{(1)*}\kappa^{(1)*}}+E_{15}^{(3)}\sqrt{\chi^{(2)*}\kappa^{(2)*}}\right)\mathscr{d}_p\right.$$
$$\left.+(-1)^\tau\left(E_{15}^{(2)}\sqrt{\chi^{(1)*}\kappa^{(1)*}}-E_{15}^{(3)}\sqrt{\chi^{(2)*}\kappa^{(2)*}}\right)\mathscr{d}_p^{-1}\right],$$

$$C_{(\tau)p}=\frac{1}{2}\left[\left(Q_{15}^{(2)}\sqrt{\chi^{(1)*}\mu^{(1)*}}+Q_{15}^{(3)}\sqrt{\chi^{(2)*}\mu^{(2)*}}\right)\mathscr{d}_p\right.$$
$$\left.+(-1)^\tau\left(Q_{15}^{(2)}\sqrt{\chi^{(1)*}\mu^{(1)*}}-Q_{15}^{(3)}\sqrt{\chi^{(2)*}\mu^{(2)*}}\right)\mathscr{d}_p^{-1}\right],$$

$$A_{(\bar{\tau})p}=\frac{1}{2}\left[\left(E_{15}^{(2)}\sqrt{\chi^{(1)*}\kappa^{(1)*}\chi^{(2)*}/\kappa^{(2)*}}+E_{15}^{(3)}\chi^{(2)*}\right)\mathscr{d}_p\right.$$
$$\left.+(-1)^{\bar{\tau}}\left(E_{15}^{(2)}\sqrt{\chi^{(1)*}\chi^{(2)*}\kappa^{(1)*}/\kappa^{(2)*}}-E_{15}^{(3)}\chi^{(2)*}\right)\mathscr{d}_p^{-1}\right],$$

$$B_{(\bar{\tau})p}=\frac{1}{2}\left[\left(\sqrt{\chi^{(2)*}\kappa^{(1)*}\kappa^{(1)*}/\kappa^{(2)*}}+\sqrt{\chi^{(2)*}\kappa^{(2)*}}\right)\mathscr{d}_p\right.$$
$$\left.+(-1)^{\bar{\tau}}\left(\sqrt{\chi^{(2)*}\kappa^{(1)*}\kappa^{(1)*}/\kappa^{(2)*}}-\sqrt{\chi^{(2)*}\kappa^{(2)*}}\right)\mathscr{d}_p^{-1}\right],$$

$$C_{(\bar{\tau})p}=\frac{1}{2}\left[\left(A_{11}^{(2)}\sqrt{\chi^{(2)*}\kappa^{(1)*}\mu^{(1)*}/\kappa^{(2)*}}+A_{11}^{(3)}\sqrt{\chi^{(2)*}\mu^{(2)*}}\right)\mathscr{d}_p\right.$$
$$\left.+(-1)^{\bar{\tau}}\left(A_{11}^{(2)}\sqrt{\chi^{(2)*}\kappa^{(1)*}\mu^{(1)*}/\kappa^{(2)*}}-A_{11}^{(3)}\sqrt{\chi^{(2)*}\mu^{(2)*}}\right)\mathscr{d}_p^{-1}\right],$$

$$A_{(\tilde{\tau})p} = \frac{1}{2}\left[\left(Q_{15}^{(2)}\sqrt{\chi^{(1)*}\chi^{(2)*}\mu^{(1)*}/\mu^{(2)*}} + Q_{15}^{(3)}\chi^{(2)*}\right)\mathscr{A}_p \right.$$
$$\left. +(-1)^{\tilde{\tau}}\left(Q_{15}^{(2)}\sqrt{\chi^{(1)*}\chi^{(2)*}\mu^{(1)*}/\mu^{(2)*}} - Q_{15}^{(3)}\chi^{(2)*}\right)\mathscr{A}_p^{-1}\right],$$

$$B_{(\tilde{\tau})p} = \frac{1}{2}\left[\left(A_{11}^{(2)}\sqrt{\chi^{(2)*}\kappa^{(1)*}\mu^{(1)*}/\mu^{(2)*}} + A_{11}^{(3)}\sqrt{\chi^{(2)*}\kappa^{(2)*}}\right)\mathscr{A}_p \right.$$
$$\left. +(-1)^{\tilde{\tau}}\left(A_{11}^{(2)}\sqrt{\chi^{(2)*}\kappa^{(1)*}\mu^{(1)*}/\mu^{(2)*}} - A_{11}^{(3)}\sqrt{\chi^{(2)*}\kappa^{(2)*}}\right)\mathscr{A}_p^{-1}\right],$$

$$C_{(\tilde{\tau})p} = \frac{1}{2}\left[\left(\sqrt{\chi^{(2)*}\mu^{(1)*}\mu^{(1)*}/\mu^{(2)*}} + \sqrt{\chi^{(2)*}\mu^{(2)*}}\right)\mathscr{A}_p \right.$$
$$\left. +(-1)^{\tilde{\tau}}\left(\sqrt{\chi^{(2)*}\mu^{(1)*}\mu^{(1)*}/\mu^{(2)*}} - \sqrt{\chi^{(2)*}\mu^{(2)*}}\right)\mathscr{A}_p^{-1}\right],$$

for $\mathscr{E}_p^{\pm} = \left(R_1^{2p} \pm R_2^{2p}\right)\big/2R_1^p R_2^p$ and $\mathscr{A}_p = R_1^p/R_2^p$; besides,

$$D_{(0)p} = D_{(2)p}D_{(3)p} - D_{(1)p}D_{(4)p}, \quad D_{(\tau)p} = A_{(2\tau+2)p}B_{(2)p} + A_{(2)p}B_{(2\tau+2)p},$$
$$D_{(\tilde{\tau})p} = A_{(2\tilde{\tau}-2)p}C_{(2)p} + A_{(2)p}C_{(2\tilde{\tau}-2)p},$$

$$D_{(i+4)p} = \left[\mathfrak{I}_i - \left(A_{(4)p}D_{(7+i)p} + A_{(6)p}D_{(10+i)p}\right)\right]\big/A_{(2)p},$$
$$D_{(i+7)p} = \left(D_{(2)p}F_{(i+3)p} - D_{(4)p}F_{(i)p}\right)\big/D_{(0)p},$$

$$D_{(i+10)p} = \left(D_{(3)p}F_{(i)p} - D_{(1)p}F_{(i+3)p}\right)\big/D_{(0)p},$$

$$F_{(i)p} = \mathfrak{I}_i B_{(2)p} + \widehat{\mathfrak{I}}_i A_{(2)p}, \quad F_{(3+i)p} = \mathfrak{I}_i C_{(2)p} + \widecheck{\mathfrak{I}}_i A_{(2)p},$$

$$G_{(1)p} = B_{(2)p}\left(\chi^{(1)*} - \chi^{(2)*}\right) - A_{(2)p}\left(E_{15}^{(2)}\sqrt{\chi^{(1)*}\kappa^{(1)*}} - E_{15}^{(3)}\sqrt{\chi^{(2)*}\kappa^{(2)*}}\right),$$
$$G_{(4)p} = \left(D_{(2)p}G_{(2)p} - G_{(1)p}D_{(4)p}\right)\big/D_{(0)p},$$

$$G_{(2)p} = C_{(2)p}\left(\chi^{(1)*} - \chi^{(2)*}\right) - A_{(2)p}\left(Q_{15}^{(2)}\sqrt{\chi^{(1)*}\mu^{(1)*}} - Q_{15}^{(3)}\sqrt{\chi^{(2)*}\mu^{(2)*}}\right),$$
$$G_{(5)p} = \left(D_{(3)p}G_{(1)p} - D_{(1)p}G_{(2)p}\right)\big/D_{(0)p},$$

$$G_{(3)p} = \left[\chi^{(1)*} - \chi^{(2)*} - A_{(4)p}G_{(4)p} - A_{(6)p}G_{(5)p}\right]\big/A_{(2)p}$$

with the vectors $(\mathfrak{I})_{3x1} = \begin{pmatrix} \chi^{(1)*} \\ E_{15}^{(2)}\sqrt{\chi^{(1)*}\kappa^{(1)*}} \\ Q_{15}^{(2)}\sqrt{\chi^{(1)*}\mu^{(1)*}} \end{pmatrix}$,

$$(\widehat{\mathfrak{I}})_{3x1} = \begin{pmatrix} -E_{15}^{(2)}\sqrt{\chi^{(1)*}\kappa^{(1)*}} \\ \kappa^{(1)*} \\ A_{11}^{(2)}\sqrt{\kappa^{(1)*}\mu^{(1)*}} \end{pmatrix}, (\widecheck{\mathfrak{I}})_{3x1} = \begin{pmatrix} -Q_{15}^{(2)}\sqrt{\chi^{(1)*}\mu^{(1)*}} \\ A_{11}^{(2)}\sqrt{\kappa^{(1)*}\mu^{(1)*}} \\ \mu^{(1)*} \end{pmatrix}$$

Appendix C

The matrices defined in Eq. (21) are presented by the form:

Appendix D

Eqs. (24) and (25) are easily transformed applying Green's theorem to the area integrals. Therefore, considering the perfect contact condition (14), the effective coefficients that appear in (24) and (25) associate with the local problem $_{\alpha 3}\mathcal{L}$ are connected by the following matricial relations:

$$\mathbf{C}_\alpha^* = K_\alpha(\delta_{\alpha 1} - i\delta_{\alpha 2}) + \sum_{s=1}^{2}\frac{\|K_\alpha\|_s}{V}\left(\int_{\Gamma_s}\mathscr{L}_3^{(2^s-1)}d\xi_2 + i\int_{\Gamma_s}\mathscr{L}_3^{(2^s-1)}d\xi_1\right)$$
$$-\varsigma\sum_{s=1}^{2}\frac{\|\widehat{K}_\alpha\|_s}{V}\left(\int_{\Gamma_s}\mathscr{M}^{(2^s-1)}d\xi_2 + i\int_{\Gamma_s}\mathscr{M}^{(2^s-1)}d\xi_1\right)$$
$$-\varsigma\sum_{s=1}^{2}\frac{\|\widecheck{K}_\alpha\|_s}{V}\left(\int_{\Gamma_s}\mathscr{N}^{(2^s-1)}d\xi_2 + i\int_{\Gamma_s}\mathscr{N}^{(2^s-1)}d\xi_1\right) \quad \text{(D1)}$$

with the vectors

$$(\mathbf{C}_\alpha^*)_{3x1} = \begin{pmatrix} C_{13\alpha 3}^* - iC_{23\alpha 3}^* \\ e_{1\alpha 3}^* - i.e_{2\alpha 3}^* \\ q_{1\alpha 3}^* - iq_{2\alpha 3}^* \end{pmatrix}, \quad (K_\alpha)_{3x1} = \begin{pmatrix} C_{\alpha 3\alpha 3} \\ e_{\alpha\alpha 3} \\ q_{\alpha\alpha 3} \end{pmatrix},$$

$$(\widehat{K}_\alpha)_{3x1} = \begin{pmatrix} e_{\alpha\alpha 3} \\ \kappa_{\alpha\alpha} \\ \alpha_{\alpha\alpha} \end{pmatrix}, \quad (\widecheck{K}_\alpha)_{3x1} = \begin{pmatrix} q_{\alpha\alpha 3} \\ \alpha_{\alpha\alpha} \\ \mu_{\alpha\alpha} \end{pmatrix} \quad \text{and} \quad (\varsigma)_{3x1} = \begin{pmatrix} -1 \\ 1 \\ 1 \end{pmatrix}.$$

$\mathscr{L}_3$, $\mathscr{M}$ and $\mathscr{N}$ are the solutions of the local problems $_{\alpha 3}\mathcal{L}$, respectively. Due to the orthogonality of the system of functions $\{e^{inx}\}_{n=-\infty}^{\infty}$ in $[0, 2\pi]$ and the Laurent's expansions of the local functions given in (18)–(20), the line integrals in (D1) are obtained analogous to Guinovart-Díaz et al., 2011 and the integrals sum are represented by

$$\int_{\Gamma_1}\mathscr{L}_3^{(1)}d\xi_2 + i\int_{\Gamma_1}\mathscr{L}_3^{(1)}d\xi_1 = \pi R_1\left[a_0 + \sum_{k=1}^{\infty}{}^o a_k\eta_{k1} + \bar{a}_1\right],$$
$$\int_{\Gamma_2}\mathscr{L}_3^{(3)}d\xi_2 + i\int_{\Gamma_2}\mathscr{L}_3^{(3)}d\xi_1 = c_1 R_2\pi,$$

$$\int_{\Gamma_1}\mathscr{M}^{(1)}d\xi_2 + i\int_{\Gamma_1}\mathscr{M}^{(1)}d\xi_1 = \pi R_1\left[b_0 + \sum_{k=1}^{\infty}{}^o b_k\eta_{k1} + \bar{b}_1\right],$$
$$\int_{\Gamma_2}\mathscr{M}^{(3)}d\xi_2 + i\int_{\Gamma_2}\mathscr{M}^{(3)}d\xi_1 = d_1 R_2\pi, \quad \text{(D2)}$$

$$\int_{\Gamma_1}\mathscr{N}^{(1)}d\xi_2 + i\int_{\Gamma_1}\mathscr{N}^{(1)}d\xi_1 = \pi R_1\left[e_0 + \sum_{k=1}^{\infty}{}^o e_k\eta_{k1} + \bar{e}_1\right],$$
$$\int_{\Gamma_2}\mathscr{N}^{(3)}d\xi_2 + i\int_{\Gamma_2}\mathscr{N}^{(3)}d\xi_1 = f_1 R_2\pi,$$

$$J = \begin{pmatrix} -\mathcal{A}_{21}(h_{11}+h_{12}) & -\mathcal{A}_{21}(h_{21}-h_{22}) & -\mathcal{B}_{21}(h_{11}+h_{12}) & -\mathcal{B}_{21}(h_{21}-h_{22}) & -\mathcal{C}_{21}(h_{11}+h_{12}) & -\mathcal{C}_{21}(h_{21}-h_{22}) \\ \mathcal{A}_{21}(h_{21}+h_{22}) & -\mathcal{A}_{21}(h_{11}-h_{12}) & \mathcal{B}_{21}(h_{21}+h_{22}) & -\mathcal{B}_{21}(h_{11}-h_{12}) & \mathcal{C}_{21}(h_{21}+h_{22}) & -\mathcal{C}_{21}(h_{11}-h_{12}) \\ -\mathcal{A}_{41}(h_{11}+h_{12}) & -\mathcal{A}_{41}(h_{21}-h_{22}) & -\mathcal{B}_{41}(h_{11}+h_{12}) & -\mathcal{B}_{41}(h_{21}-h_{22}) & -\mathcal{C}_{41}(h_{11}+h_{12}) & -\mathcal{C}_{41}(h_{21}-h_{22}) \\ \mathcal{A}_{41}(h_{21}+h_{22}) & -\mathcal{A}_{41}(h_{11}-h_{12}) & \mathcal{B}_{41}(h_{21}+h_{22}) & -\mathcal{B}_{41}(h_{11}-h_{12}) & \mathcal{C}_{41}(h_{21}+h_{22}) & -\mathcal{C}_{41}(h_{11}-h_{12}) \\ -\mathcal{A}_{61}(h_{11}+h_{12}) & -\mathcal{A}_{61}(h_{21}-h_{22}) & -\mathcal{B}_{61}(h_{11}+h_{12}) & -\mathcal{B}_{61}(h_{21}-h_{22}) & -\mathcal{C}_{61}(h_{11}+h_{12}) & -\mathcal{C}_{61}(h_{21}-h_{22}) \\ \mathcal{A}_{61}(h_{21}+h_{22}) & -\mathcal{A}_{61}(h_{11}-h_{12}) & \mathcal{B}_{61}(h_{21}+h_{22}) & -\mathcal{B}_{61}(h_{11}-h_{12}) & \mathcal{C}_{61}(h_{21}+h_{22}) & -\mathcal{C}_{61}(h_{11}-h_{12}) \end{pmatrix},$$

$$\tilde{E}_p = \begin{pmatrix} \mathcal{A}_{1p} & 0 & \mathcal{B}_{1p} & 0 & \mathcal{C}_{1p} & 0 \\ 0 & \mathcal{A}_{1p} & 0 & \mathcal{B}_{1p} & 0 & \mathcal{C}_{1p} \\ \mathcal{A}_{3p} & 0 & \mathcal{B}_{3p} & 0 & \mathcal{C}_{3p} & 0 \\ 0 & \mathcal{A}_{3p} & 0 & \mathcal{B}_{3p} & 0 & \mathcal{C}_{3p} \\ \mathcal{A}_{5p} & 0 & \mathcal{B}_{5p} & 0 & \mathcal{C}_{5p} & 0 \\ 0 & \mathcal{A}_{5p} & 0 & \mathcal{B}_{5p} & 0 & \mathcal{C}_{5p} \end{pmatrix}, \quad W_{kp} = \begin{pmatrix} -\mathcal{A}_{2p}w_{1kp} & \mathcal{A}_{2p}w_{2kp} & -\mathcal{B}_{2p}w_{1kp} & \mathcal{B}_{2p}w_{2kp} & -\mathcal{C}_{2p}w_{1kp} & \mathcal{C}_{2p}w_{2kp} \\ \mathcal{A}_{2p}w_{2kp} & \mathcal{A}_{2p}w_{1kp} & \mathcal{B}_{2p}w_{2kp} & \mathcal{B}_{2p}w_{1kp} & \mathcal{C}_{2p}w_{2kp} & \mathcal{C}_{2p}w_{1kp} \\ -\mathcal{A}_{4p}w_{1kp} & \mathcal{A}_{4p}w_{2kp} & -\mathcal{B}_{4p}w_{1kp} & \mathcal{B}_{4p}w_{2kp} & -\mathcal{C}_{4p}w_{1kp} & \mathcal{C}_{4p}w_{2kp} \\ \mathcal{A}_{4p}w_{2kp} & \mathcal{A}_{4p}w_{1kp} & \mathcal{B}_{4p}w_{2kp} & \mathcal{B}_{4p}w_{1kp} & \mathcal{C}_{4p}w_{2kp} & \mathcal{C}_{4p}w_{1kp} \\ -\mathcal{A}_{6p}w_{1kp} & \mathcal{A}_{6p}w_{2kp} & -\mathcal{B}_{6p}w_{1kp} & \mathcal{B}_{6p}w_{2kp} & -\mathcal{C}_{6p}w_{1kp} & \mathcal{C}_{6p}w_{2kp} \\ \mathcal{A}_{6p}w_{2kp} & \mathcal{A}_{6p}w_{1kp} & \mathcal{B}_{6p}w_{2kp} & \mathcal{B}_{6p}w_{1kp} & \mathcal{C}_{6p}w_{2kp} & \mathcal{C}_{6p}w_{1kp} \end{pmatrix}$$

The following equations (D2) are obtained setting in (21) for $p = 1$, $\alpha = 1$ and $\alpha = 2$, respectively, according to the problem $_{\alpha 3}\mathcal{L}$ to be solved. They are necessary in order to obtain analytical expressions for the effective coefficients.

$$\tilde{\Delta}_i = V_3 \frac{R_1^2 - R_2^2}{2R_1R_2}(\mathcal{K}_{i1}\mathcal{G}_1 + \mathcal{K}_{i2}\mathcal{G}_2 + \mathcal{K}_{i3}\mathcal{G}_3),$$

where F_{1i}, F_{2i}, F_{3i} and $\tilde{\Delta}_i$, $i = 1, 2, 3$ are constants denoted in this form in order to simplify the notation. Moreover,

$$(\mathcal{A})_{3x1} = \begin{pmatrix} \mathcal{A}_{11} \\ \mathcal{B}_{11} \\ \mathcal{C}_{11} \end{pmatrix}, \quad \mathcal{G} = \begin{pmatrix} G_{(3)1} \\ G_{(4)1} \\ G_{(5)1} \end{pmatrix}, \quad (\mathcal{S})_{3x3} = \begin{pmatrix} \chi^{(1)*} - 1 & E_{15}^{(2)}\sqrt{\chi^{(1)*}\kappa^{(1)*}} - E_{15}^{(1)} & Q_{15}^{(2)}\sqrt{\chi^{(1)*}\mu^{(1)*}} - Q_{15}^{(1)} \\ E_{15}^{(2)}\sqrt{\chi^{(1)*}\kappa^{(1)*}} - E_{15}^{(1)} & \kappa^{(1)*} - 1 & A_{11}^{(2)}\sqrt{\kappa^{(1)*}\mu^{(1)*}} - A_{11}^{(1)} \\ Q_{15}^{(2)}\sqrt{\chi^{(1)*}\mu^{(1)*}} - Q_{15}^{(1)} & A_{11}^{(2)}\sqrt{\kappa^{(1)*}\mu^{(1)*}} - A_{11}^{(1)} & \mu^{(1)*} - 1 \end{pmatrix},$$

$$\mathcal{K} = \begin{pmatrix} \chi^{(2)*} - \chi^{(1)*} & E_{15}^{(3)}\chi^{(2)*} - E_{15}^{(2)}\sqrt{\chi^{(2)*}\chi^{(1)*}\kappa^{(1)*}/\kappa^{(2)*}} & Q_{15}^{(3)}\chi^{(2)*} - Q_{15}^{(2)}\sqrt{\chi^{(2)*}\chi^{(1)*}\mu^{(1)*}/\mu^{(2)*}} \\ E_{15}^{(3)}\sqrt{\chi^{(2)*}\kappa^{(2)*}} - E_{15}^{(2)}\sqrt{\chi^{(1)*}\kappa^{(1)*}} & \sqrt{\chi^{(2)*}\kappa^{(1)*}\kappa^{(1)*}/\kappa^{(2)*}} - \sqrt{\chi^{(2)*}\kappa^{(2)*}} & A_{11}^{(2)}\sqrt{\chi^{(2)*}\kappa^{(1)*}\mu^{(1)*}/\mu^{(2)*}} - A_{11}^{(3)}\sqrt{\chi^{(2)*}\kappa^{(2)*}} \\ Q_{15}^{(3)}\sqrt{\chi^{(2)*}\mu^{(2)*}} - Q_{15}^{(2)}\sqrt{\chi^{(1)*}\mu^{(1)*}} & A_{11}^{(2)}\sqrt{\chi^{(2)*}\kappa^{(1)*}\mu^{(1)*}/\kappa^{(2)*}} - A_{11}^{(3)}\sqrt{\chi^{(2)*}\mu^{(2)*}} & \sqrt{\chi^{(2)*}\mu^{(1)*}\mu^{(1)*}/\mu^{(2)*}} - \sqrt{\chi^{(2)*}\mu^{(2)*}} \end{pmatrix},$$

$$\mathcal{A}_{21}\left[a_0 + \sum_{k=1}^{\infty}{}^o a_k\eta_{k1}\right] + \mathcal{B}_{21}\left[b_0 + \sum_{k=1}^{\infty}{}^o b_k\eta_{k1}\right] + \mathcal{C}_{21}\left[e_0 + \sum_{k=1}^{\infty}{}^o e_k\eta_{k1}\right]$$
$$+ \mathcal{A}_{11}\,\bar{a}_1 + \mathcal{B}_{11}\,\bar{b}_1 + \mathcal{C}_{11}\,\bar{e}_1 = \mathcal{T}_{11}[\delta_{\alpha 1} - i\delta_{\alpha 2}],$$

$$\mathcal{A}_{41}\left[a_0 + \sum_{k=1}^{\infty}{}^o a_k\eta_{k1}\right] + \mathcal{B}_{41}\left[b_0 + \sum_{k=1}^{\infty}{}^o b_k\eta_{k1}\right] + \mathcal{C}_{41}\left[e_0 + \sum_{k=1}^{\infty}{}^o e_k\eta_{k1}\right]$$
$$+ \mathcal{A}_{31}\,\bar{a}_1 + \mathcal{B}_{31}\,\bar{b}_1 + \mathcal{C}_{31}\,\bar{e}_1 = \mathcal{T}_{21}[\delta_{\alpha 1} - i\delta_{\alpha 2}], \qquad\text{(D3)}$$

$$\mathcal{A}_{61}\left[a_0 + \sum_{k=1}^{\infty}{}^o a_k\eta_{k1}\right] + \mathcal{B}_{61}\left[b_0 + \sum_{k=1}^{\infty}{}^o b_k\eta_{k1}\right] + \mathcal{C}_{61}\left[e_0 + \sum_{k=1}^{\infty}{}^o e_k\eta_{k1}\right]$$
$$+ \mathcal{A}_{51}\,\bar{a}_1 + \mathcal{B}_{51}\,\bar{b}_1 + \mathcal{C}_{51}\,\bar{e}_1 = \mathcal{T}_{31}[\delta_{\alpha 1} - i\delta_{\alpha 2}],$$

then, by means of the relations defined in Wang and Ding (2006) (Appendix A), substituting the expression of (D2) into (D1) and using the corresponding solution of (D3), and the analytical solution of c_1, d_1 and f_1 obtained of (B.1), (B.2) and (B.6)–(B.8) system a simple analytical formulae for the effective properties are deduced depending only the unknowns $\bar{a}_1$, $\bar{b}_1$ and $\bar{e}_1$ as it is represented in (26) and (27). The magnitudes that appear in (26) and (27) corresponding to the local problem $_{\alpha 3}\mathcal{L}$ can be summarized as follows:

$$\Upsilon_i = F_{i1} + \varsigma_1 F_{11}\mathcal{A}_i/\mathcal{A}_{21} + \varsigma_2(F_{21} - F_{11}\mathcal{B}_{21}/\mathcal{A}_{21})$$
$$\times [H_{1i+4} - H_{12}J_{1i+1}/J_{11}]/H_{11} + \varsigma_2(F_{31} - F_{11}\mathcal{C}_{21}/\mathcal{A}_{21})J_{1i+1}/J_{11},$$

$$\Upsilon_{i+3} = F_{i2} + \varsigma_i F_{12}\mathcal{A}_i/\mathcal{A}_{21} + \varsigma_i(F_{22} + F_{12}\mathcal{B}_{21}/\mathcal{A}_{21})$$
$$\times [H_{1i+4} - H_{12}J_{1i+1}/J_{11}]/H_{11} + \varsigma_i(F_{32} + F_{12}\mathcal{C}_{21}/\mathcal{A}_{21})J_{1i+1}/J_{11},$$

$$\Upsilon_{i+6} = F_{i3} + \varsigma_i F_{13}\mathcal{A}_i/\mathcal{A}_{21} + \varsigma_i(F_{23} + F_{13}\mathcal{B}_{21}/\mathcal{A}_{21})$$
$$\times [H_{1i+4} - H_{12}J_{1i+1}/J_{11}]/H_{11} + \varsigma_i(F_{33} + F_{13}\mathcal{C}_{21}/\mathcal{A}_{21})J_{1i+1}/J_{11},$$

$$\Delta_i = \tilde{\Delta}_i + [F_{1i}H_{11} - F_{1i}\mathcal{B}_{21}\mathcal{A}_{41} - \varsigma_i F_{2i}\mathcal{A}_{21}\mathcal{A}_{41}](\mathcal{T}_{11}/\mathcal{A}_{21}H_{11})$$
$$+ [F_{1i}\mathcal{B}_{21} + \varsigma_i F_{2i}\mathcal{A}_{21}](\mathcal{T}_{21}/H_{11})$$
$$+ [(\mathcal{B}_{21}H_{12} - \mathcal{C}_{21}H_{11})(F_{1i}/\mathcal{A}_{21}H_{11})$$
$$+ \varsigma_i F_{2i}H_{12}/H_{11} - \varsigma_i F_{3i}](J_{15}/J_{11}),$$

$$F_{i1} = \mathcal{S}_{i1}((V_2 + V_3)/R_1) + [D_{(4+i)1}\mathcal{K}_{11} + D_{(7+i)1}\mathcal{K}_{12} + D_{(10+i)1}\mathcal{K}_{13}]$$
$$\times (V_3/R_2),$$

$$F_{i2} = \mathcal{S}_{i2}((V_2 + V_3)/R_1) - \varsigma_i[D_{(4+i)1}\mathcal{K}_{21} + D_{(7+i)1}\mathcal{K}_{22} + D_{(10+i)1}\mathcal{K}_{23}]$$
$$\times (V_3/R_2),$$

$$F_{i3} = \mathcal{S}_{i3}((V_2 + V_3)/R_1) - \varsigma_i[D_{(4+i)1}\mathcal{K}_{31} + D_{(7+i)1}\mathcal{K}_{32} + D_{(10+i)1}\mathcal{K}_{33}]$$
$$\times (V_3/R_2),$$

$$H_{11} = (\mathcal{A}_{41}\mathcal{B}_{21} - \mathcal{A}_{21}\mathcal{B}_{41}), \quad H_{12} = (\mathcal{A}_{41}\mathcal{C}_{21} - \mathcal{A}_{21}\mathcal{C}_{41}),$$
$$H_{13} = (\mathcal{A}_{61}\mathcal{B}_{21} - \mathcal{A}_{21}\mathcal{B}_{61}), \quad H_{14} = (\mathcal{A}_{61}\mathcal{C}_{21} - \mathcal{A}_{21}\mathcal{C}_{61}),$$

$$H_{15} = (\mathcal{A}_{21}\mathcal{A}_{31} - \mathcal{A}_{11}\mathcal{A}_{41}), \quad H_{18} = (\mathcal{A}_{21}\mathcal{A}_{51} - \mathcal{A}_{11}\mathcal{A}_{61}),$$
$$H_{16} = (\mathcal{A}_{21}\mathcal{B}_{31} - \mathcal{A}_{41}\mathcal{B}_{11}), \quad H_{17} = (\mathcal{A}_{21}\mathcal{C}_{31} - \mathcal{A}_{41}\mathcal{C}_{11}),$$

$$H_{19} = (\mathcal{A}_{21}\mathcal{B}_{51} - \mathcal{A}_{61}\mathcal{B}_{11}), \quad H_{20} = (\mathcal{A}_{21}\mathcal{C}_{51} - \mathcal{A}_{61}\mathcal{C}_{11}),$$
$$J_{11} = (H_{12}H_{13} - H_{11}H_{14}), \quad J_{12} = (H_{15}H_{13} - H_{11}H_{18}),$$

$$J_{13} = (H_{16}H_{13} - H_{11}H_{19}), \quad J_{14} = (H_{17}H_{13} - H_{11}H_{20}),$$
$$J_{15} = (H_{13}(\mathcal{A}_{41}\mathcal{T}_{11} - \mathcal{A}_{21}\mathcal{T}_{21}) - H_{11}(\mathcal{A}_{61}\mathcal{T}_{11} - \mathcal{A}_{21}\mathcal{T}_{31})).$$

References

Aboudi, J., 2001. Micromechanical analysis of fully coupled electro-magneto-thermo-elastic multiphase composites. Smart Mater. Struct. 10, 867–877.

Benveniste, Y., 1987. A new approach to the application of Mori–Tanaka's theory in composite materials. Mech. Mater. 6, 147–157.

Benveniste, Y., 1995. Magnetoelectric effect in fibrous composites with piezoelectric and piezomagnetic phases. Phys. Rev. B 51, 16424–16427.

Benveniste, Y., Dvorak, G.J., 1992. Uniform fields and universal relation in piezoelectric composites. J. Mech. Phys. Solids 44, 1295–1312.

Bichurin, M.I., Filippov, D.A., Petrov, V.M., Laletsin, V.M., Paddubnaya, N., Srinivasan, G., 2003a. Resonance magnetoelectric effects in layered magnetostrictive-piezoelectric composites. Phys. Rev. B 68, 132408.

Bichurin, M.I., Petrov, V.M., Srinivasan, G., 2003b. Theory of low-frequency magnetoelectric coupling in magnetostrictive-piezoelectric bilayers. Phys. Rev. B 68, 054402.

Bracke, L.P.M., Van Vliet, R.G., 1981. Broadband magneto-electric transducer using a composite material. Int. J. Electron. 51 (3), 255–262.

Bravo-Castillero, J., Rodríguez-Ramos, R., Mechkour, H., Otero, J.A., Sabina, F.J., 2008. Homogenization of magneto-electro-elastic multilaminated materials. Q. J. Mech. Appl. Math. 61, 311–332.

Bravo-Castillero, J., Rodríguez-Ramos, R., Guinovart-Díaz, R., Sabina, F.J., Aguiar, A.R., Silva, U.P., Gómez-Muñoz, J.L., 2009. Analytical formulae for electromechanical effective properties of 3-1 longitudinally porous piezoelectric materials. Acta Mater. 57, 795–803.

Bravo-Castillero, J., Guinovart-Díaz, R., Rodríguez-Ramos, R., Mechkour, H., Brenner, R., Camacho-Montes, H., Sabina, F.J., 2012. Universal Relations and Effective Coefficients of Magneto-Electro-Elastic Perforated Structures. Quarterly Journal of Mechanics & Applied Mathematics. 65, 51–85.

Budiansky, B., 1965. On the elastic moduli of some heterogeneous materials. J. Mech. Phys. Solids 13 (4), 223–227.

Camacho-Montes, H., Rodríguez-Ramos, R., Bravo-Castillero, J., Guinovart-Díaz, R., Sabina, F.J., 2006. Effective coefficients for two phase magneto-electroelastic fibrous composite with square symmetry cell in plane mechanical displacement and out-of-plane electric and magnetic field case. Integr. Ferroelect. 83, 49–65.

Camacho-Montes, H., Sabina, F.J., Bravo-Castillero, J., Guinovart-Díaz, R., Rodríguez-Ramos, R., 2009. Magnetoelectric coupling and cross-property connections in a square array of a binary composite. Int. J. Eng. Sci. 47, 294–312.

Chen, T.Y., 1993. Piezoelectric properties of multiphase fibrous composites: some theoretical results. J. Mech. Phys. Solids 41, 1781–1794.

Dinzart, F., Sabar, H., 2011. Magneto-electro-elastic coated inclusion problem and its application to magnetic-piezoelectric composite materials. Int. J. Solids Struct. 48, 2393–2401.

Eshelby, J.D., 1957. The determination of the elastic field of an ellipsoidal inclusion, and related problems. Proc. R. Soc. London Ser. A 241, 376–396.

Espinosa-Almeyda, Y., López-Realpozo, J.C., Rodríguez-Ramos, R., Bravo-Castillero, J., Guinovart-Díaz, R., Camacho-Montes, H., Sabina, F.J., 2011. Effects of interface contacts on the magneto electro-elastic coupling for fiber reinforced. Int. J. Solids Struct. 48, 1525–1533.

Feng, W.J., Pan, E., Wang, W., Gazonas, G.A., 2009. A second-order theory for magnetoelectroelastic materials with transverse isotropy. Smart Mater. Struct. 18, 025001.

Fuentes, L., García, M., Bueno, D., Fuentes, M.E., Muñoz, A., 2006. Magnetoelectric effect in $Bi_5Ti_3FeO_{15}$ ceramics obtained by molten salts synthesis. Ferroelectrics 336, 81–89.

Guinovart-Díaz, R., Rodríguez-Ramos, R., Bravo-Castillero, J., Sabina, F.J., Camacho-Montes, H., 2008. Electro-mechanical moduli of three-phase fiber composites. Mater. Lett. 62, 2385–2387.

Guinovart-Díaz, R., López-Realpozo, J.C., Rodríguez-Ramos, R., Bravo-Castillero, J., Ramírez, M., Camacho-Montes, H., Sabina, F.J., 2011. Influence of parallelogram cells in the axial behaviour of fibrous composite. Int. J. Eng. Sci. 49, 75–84.

Guinovart-Díaz, R., Yan, P., Rodríguez-Ramos, R., López-Realpozo, J.C., Jiang, C.P., Bravo-Castillero, J., Sabina, F.J., 2012. Effective properties of piezoelectric composites with parallelogram periodic cell. Int. J. Eng. Sci. 53, 58–66.

Guinovart-Díaz, R., Rodríguez-Ramos, R., Bravo-Castillero, J., Sabina, F.J., Monsivais Galindo, G., Wang, Yue-Sheng, 2013. Plane magneto-electro-elastic moduli of fiber composites with interphase. Mech. Adv. Mater. Struct. 20, 552–563.

Jiang, C.P., Xu, Y.L., Cheung, Y.K., Lo, S.H., 2004. A rigorous analytical method for doubly periodic cylindrical inclusions under longitudinal shear and its application. Mech. Mater. 36, 225–237.

Kuo, H.Y., 2011. Multicoated elliptic fibrous composites of piezoelectric and piezomagnetic phases. Int. J. Eng. Sci. 49, 561–575.

Kuo, H.Y., Pan, E., 2011. Effective magnetoelectric effect in multicoated circular fibrous multiferroic composites. J. Appl. Phys. 109, 104901.

Landau, L.D., Lifshitz, E.M., 1960. Electrodynamics of Continuous Media. Pergamon, Oxford, p. 119 (translation of Russian ed., 1958).

Lee, J., Boyd IV, J.G., Lagoudas, D.C., 2005. Effective properties of three-phase electro-magneto-elastic composites. Int. J. Eng. Sci. 43, 790–825.

Li, J.Y., 2000. Magnetoelectroelastic multi-inclusion and inhomogeneity problems and their applications in composite materials. Int. J. Eng. Sci. 38 (18), 1993–2011.

Li, J.Y., Dunn, M.L., 1998. Micromechanics of magnetoelectroelastic composite materials: average fields and effective behavior. J. Intell. Mater. Syst. Struct. 9, 404–416.

Lin, Y., Cai, N., Zhai, J., Liu, G., Ce-Wen, N., 2005. Giant magnetoelectric effect in multiferroic laminated composites. Phys. Rev. B 72, 012405.

López-López, E., Sabina, F.J., Bravo-Castillero, J., Guinovart-Díaz, R., Rodríguez-Ramos, R., 2005. Overall electromechanical properties of a binary composite with 622 symmetry constituents. Antiplane shear piezoelectric state. Int. J. Solids Struct. 42, 5765–5777.

Luo, H.A., Weng, G.J., 1987. On Eshelby's inclusions problem in a three-phase spherically concentric solid, and a modification of Mori–Tanaka's method. Mech. Mater. 6, 347–361.

Mclaughlin, R., 1977. A study of the differential scheme for composite masterials. Int. J. Eng. Sci. 15 (4), 237–244.

Mori, T., Tanaka, K., 1973. Average stress in matrix and average elastic energy of materials with misfitting inclusions. Acta Metall. Sin. 21, 571–574.

Nan, C.W., 1994. Magnetoelectric effect in composites of piezoelectric and piezomagnetic phases. Phys. Rev. B 50, 6082–6088.

Parton, V.Z., Kudryavtsev, B.A., 1993. Engineering Mechanics of Composite Materials. CRC Press, Boca Raton.

Petrov, V.M., Srinivasan, G., Bichurin, M.I., Gupta, A., 2007a. Theory of magnetoelectric effects in ferrite piezoelectric nanocomposites. Phys. Rev. B 75, 224407.

Petrov, V.M., Srinivasan, G., Laletsin, U., Bichurin, M.I., Tuskov, D.S., Paddubnaya, N., 2007b. Magnetoelectric effects in porous ferromagnetic-piezoelectric bulk composites: experiment and theory. Phys. Rev. B 75, 174422.

Pobedrya, B.E., 1984. Mechanics of Composite Materials. Moscow State University Press (in Russian).

Rodríguez-Ramos, R., Sabina, F.J., Guinovart-Díaz, R., Bravo-Castillero, J., 2001. Closed-form expressions for the effective coefficients of a fiber-reinforced composite with transversely isotropic constituents – I. Elastic and square symmetry. Mech. Mater. 33, 223–235.

Rodríguez-Ramos, R., Yan, P., López-Realpozo, J.C., Guinovart-Díaz, R., Bravo-Castillero, J., Sabina, F.J., Jiang, C.P., 2011. Two analytical models for the study of periodic fibrous elastic composite with different unit cell. Compos. Struct. 93, 709–714.

Singh, A., Pandey, V., Kotnala, R.K., Pandey, D., 2008. Direct Evidence for Multiferroic Magnetoelectric Coupling in $0.9BiFeO_3–0.1BaTiO_3$. Phys. Rev. Lett. 101, 247602.

Sixto-Camacho, L.M., Bravo-Castillero, J., Brenner, R., Guinovart-Díaz, R., Mechkour, H., Rodríguez-Ramos, R., Sabina, F.J., 2013. Asymptotic homogenization of periodic thermo-magneto-electro-elastic heterogeneous media. Comput. Math. Appl. 66, 2056–2074.

Srinivas, S., Li, J.Y., 2005. The effective magnetoelectric coefficients of polycrystalline multiferroic composites. Acta Mater. 53, 4142–4153.

Srinivas, S., Li, J.Y., Zhou, Y.C., Soh, A.K., 2006. The effective magnetoelectroelastic moduli of matrix-based multiferroic composites. J. Appl. Phys. 99, 043905.

Tong, Z.H., Lo, S.H., Jiang, C.P., Cheung, Y.K., 2008. An exact solution for the three-phase thermo-electro-magneto-elastic cylinder model and its application to piezoelectric–magnetic fiber composites. Int. J. Solids Struct. 45, 5205–5219.

Van Suchtelen, J., 1972. Product properties: a new application of composite materials. Philips Res. Rep. 27, 28–37.

Wang, H.M., Ding, H.J., 2006. Transient responses of a magneto-electro-elastic hollow sphere for fully coupled spherically symmetric problem. Eur. J. Mech. A. Solids 25, 965–980.

Wang, X., Pan, E., 2007. Magnetoelectric effects in multiferroic fibrous composite with imperfect interface. Phys. Rev. B 76, 214107.

Wang, J., Duan, H.L., Zhang, Z., Huang, Z.P., 2005. An anti-interpenetration model and connections between interphase and interface models in particle-reinforced composites. Int. J. Mech. Sci. 47, 701–718.

Yan, P., Jiang, C.P., Song, F., 2011. An eigenfunction expansion-variational method for the anti-plane electroelastic behavior of three-phase fiber composites. Mech. Mater. 43, 586–597.

Yan, P., Jiang, C.P., Song, F., 2013. Unified series solution for the anti-plane effective magnetoelectroelastic moduli of three-phase fiber composites. Int. J. Solids Struct. 50, 176–185.

Zhang, Z.K., Soh, A.K., 2005. Micromechanics predictions of the effective moduli of magnetoelectroelastic composite materials. Eur. J. Mech. A Solids 24, 1054–1067.